

Final Report for 2021-2025

Isotope Monitoring and Water Balance Assessment of the St. Mary and Milk River basins

Submitted to the International Watershed Initiatives (IWI) Program

Prepared by Dr. Tricia Stadnyk, P.Eng.
7-31-2025

Table of Contents

List of Figures	ii
List of Tables	iii
Contributors	iv
Scope & Objectives	1
Deliverables & Timelines	1
1. Monitoring Network.....	2
Long-term Plan for Monitoring Network	5
2. Isotope & Hydrologic Modelling.....	5
2.1. Hydrometeorological Analysis	5
2.1.1. Isotope in Precipitation Forcing.....	6
2.2. Landscape Analysis – Non-Contributing Areas	7
2.3. Hydrological Modelling.....	8
2.4. Model Agnostic Isotope Tracer (MAIT) Modelling.....	8
2.4.1. Model Setup Methods.....	8
2.4.2. MAITsim Model Results.....	9
2.5. Fully Coupled Isotope-Hydrological Modelling	12
3. Source Separation	13
3.1. Isotope Framework	13
3.2. EMMA Modelling	18
3.2.1. Groundwater (Baseflow) Analysis	20
3.2.2. Diversion Inflow Analysis	23
3.3. Water Balance Assessment	26
4. Summary of Findings.....	30
4.1. Gaps in Knowledge.....	31
5. Recommendations.....	31
5.1. Value of Isotopes Monitoring.....	31
5.2. Sustaining an Isotope Monitoring Network	32
5.3. Isotope-Hydrological Modelling.....	33
6. Data Availability	34
7. References	34

List of Figures

Figure 1. Map of streamflow isotope samples collected by UC-HAL, Water Survey of Canada and United States Geological Survey from 2022 to 2024, including frequency of sampling per location.....	3
Figure 2. Streamflow-isotope timeseries from 2016-2024 developed from this IWI research.	5
Figure 3. Summary of meteorological conditions obtained from NARR for the study period from January 2016 to December 2024, including modelled isotopes in precipitation signatures required for water balance modelling.	6
Figure 4. Spatial variability of the isotopes in precipitation input across the Milk River basin as predicted by iso P (2016-2024).....	7
Figure 5. Map of prairie potholes with a 2-year return period; maps were generated for 2-, 5-, and 10-year return periods and are available for the SMM study region.	8
Figure 6. HYPE model storages for a single sub-basin, with the ‘baseflow’ source highlighted in green	9
Figure 7. Isotope-isotope framework comparing HYPE-MAITsim simulated evaporatively enriched values relative to observed isotope observations collected during the simulation period (2016-2018).....	10
Figure 8. Observed and simulated (a) hydrographs and (b) isotographs at 11AA025.	10
Figure 9. Daily average annual hydrographs (top) and isographs (bottom)for the Milk River headwaters (11AA025).	11
Figure 10. Simulated relative to observed isotope framework for the Milk River basin at AB11AA0280 (no diversion included in the model), derived by HYPE-CHARM fusion model (uncalibrated).....	13
Figure 11. Long-term isotope framework developed from all samples (2016-2024) with flux-weighted end points. End points provided in Table 4.	15
Figure 12. Isotope framework by (a) river or tributary input, and (b) for the Milk River basin only by year. Note axis scale differences.....	16
Figure 13. St. Mary and Milk River local mixing lines (2017-2024) relative to limiting enrichment (δ^*) and steady state isotopic composition (δ_s) for the Milk (orange) and St. Mary (purple) rivers.	17
Figure 14. Groundwater (baseflow) separation using EMMA approach in streamwise direction from all samples (2018-2023) relative to 2020 (no diversion); 2020 included only two samples from end of September and early October. IQR boxes are 25/75 with median value, whiskers are 10/90 with outliers at 1.5xIQR.	21
Figure 15. Daily average annual timeseries separation of HYPE simulated baseflow relative to total flow.	22

Figure 16. HYPE simulated baseflow fraction from March to October for the entire period of simulation for the headwater basin, 11AA025. 22

Figure 17. Groundwater simulated and observed relative to precipitation input. 23

Figure 18. EMMA mixing regime for water isotopes collected from different SMM source waters. The gray region denotes the mixing regime; end points are denoted by 1, 2 and 3 (red numbers). Solid markers represent all data, while hollow represent diversion-affected only (May to September). 24

Figure 19. Basin relative water loss derived from isotope-water balance for (a) T/ET, and (b) E/I. Red dashed line represents maximum T/ET physically possible (ratio of 1). Negative values for T/ET and E/I are not physically possible and represent higher local inflow than total inflow, likely resulting from irrigation withdrawals and returns. 29

List of Tables

Table 1. Updated project timeline. Green represents task completion, yellow in-progress and white/blank not complete. 1

Table 2. Summary of streamflow sampling undertaken from 2022 to 2024, separated by whether samples were taken as part of the UC-HAL longitudinal river surveys or as part of monthly river sampling (routine point sampling) at significant Water Survey of Canada (WSC) and United States Geological Survey (USGS) hydrometric stations: 11AA001, 11AA005, 11AA025, and 11AA031. 2

Table 3. Summary of streamflow sampling undertaken from 2020 to 2024, separated into the four subbasin categories used in EMMA modelling, plus an additional category capturing tributaries and springs (as part of investigating additional source inputs) that are not part of the main stem Milk River. Counted samples include those taken from the corresponding WSC gauge in that area plus those in the same location category that were taken as part of the UC-HAL longitudinal river surveys. 3

Table 4. End points from long-term framework derived from samples collected 2016-2024, by river basin. 15

Table 5. Local mixing line (LML) equation of best fit (linear) by river in the SMM, where $Y = \delta^2H$ and $X = \delta^{18}O$ based on period stated 16

Table 6. Comparison of estimated S_{LEL} based on different methods and end points. 18

Table 7. Gauges where EMMA was performed; basin IDs correspond to those delineated on Figure 1. *Gauges where natural flows are estimated for the treaty. 20

Table 8. Summary of EMMA endmembers identified in the study using data from 2016-2024, corresponding to Figure 18. 23

Table 9. EMMA results, estimating the contribution of diversion inflow from the St. Mary to total streamflow relative to a second endmember while the diversion is active. HW = Milk headwater (11AA025), GW = groundwater endpoint, Milk-East = 11AA031, Milk@Milk = 11AA005. 25

Table 10. Water balance assessment summary for average annual basin water yield, E/I and T/ET estimates by year and overall (2016-2024). Basin IDs 3 and 4 are local water balance only (excludes upstream inflows). Dashes represent insufficient data to complete calculations. 28

Table 11. Base isotope monitoring sample collection schedule, viable to be supported by WSC/USGS, and associated cost estimate for 2025 and beyond. 32

Contributors

Many researchers have contributed to the data collection, water sample analyses, and data compilation and numerical analyses undertaken for the following study. The following individuals are acknowledged for their contributions to this study and report:

- Terri Whitehead
- Randy Fagan
- Bailey Knapp
- Mya Lyse
- Paul Harrop
- Paul Coderre
- Dayal Wijayarathne
- Anthony Kroll
- Tegan Holmes
- Alain Pietroniro
- Water Survey of Canada, Calgary office
- US Geological Survey, Montana Office

Scope & Objectives

To develop a long-term stable isotope of water monitoring network in the St. Mary and Milk River (SMM) basins, underpinned by coupled hydrologic-isotope modelling of the St. Mary and Milk River basins, to examine changing hydrologic-isotope water balance conditions and source water contributions.

This research will continue the work funded under SMM-01-2021 to establish a critical long-term isotope monitoring network for the Milk and St. Mary River basins in an endeavour to provide an independent means of estimating diverted flow, impact of diverted water on downstream Milk River water balance, and a means of continual basin water supply assessment.

Deliverables & Timelines

The following key deliverables were identified in the project proposal and are here within reported on:

1. Establish a long-term stable isotope monitoring network in the SMM basins that supports source water separation and identification.
2. Apply a coupled isotope-hydrologic model of the SMM basins to continuously simulate isotopic separations and source water signatures.
3. Assess water balance and source water separations for SMM basins under various climatic and diversion scenarios.

The following is an update on the status of our deliverables. A four-month extension to the MOU was requested by the University of Calgary team and granted by IJC, moving the project completion date to July 31, 2025. The project is on-track with this new timeline, with all originally proposed tasks anticipated to be fulfilled (Table 1).

Table 1. Updated project timeline. Green represents task completion, yellow in-progress and white/blank not complete.

Task ID	Completion Date	Task(s)	Status
1	2022-12-01	Establish isotope monitoring network	
	2023-03-31	Initiate consistent isotope sampling program within SMM basins	
2	2023-03-31	Update isotope framework #1 (add 2020-2021 data)	
	2023-03-01	Identification of significant endmembers and evaluation of water balance components	
3	2023-03-01	Develop isotope modelling framework (MAITsim)	
	2023-03-01	Testing and evaluation of isotope modelling framework	
4	2023-03-01	Update to isotope framework #2 (add 2022 data)	
	2023-09-01	Identify significant changes in endmembers or storage/fluxes	
5	2023-03-01	Water balance assessment (EMMA modelling)	
	2024-03-31	Groundwater separations, E/I, T/ET modelling	
	2024-08-01	Finalize model agnostic isotope tracer code (MAITsim), code release	
6	2024-03-01	Update isotope framework #3 (add 2023 data)	
	2024-09-31	Preparation of climate scenarios, prairie pothole routine for HYPE	

	2024-12-31	HYPE hydrological modelling of SMM	
7	2024-12-31	Draft peer review publication on isotope network in SMM	
	2024-12-31	Draft peer review publication on isotope modelling in SMM	
8	2025-03-01	Update isotope framework #4 (add 2024 data)	
	2025-05-30	Numerical simulation of isotope modelling (MAITsim) complete	
	2025-07-31	Submission of manuscripts	Aug 31, 2025
	2025-07-31	Final report issued to IJC	

Results from items reported as complete (green) are included in this final report. Outstanding items (yellow) have completion dates noted.

1. Monitoring Network

The following sampling resolution was targeted to provide the most complete coverage for IHS and source estimation:

- *Groundwater*: 2 or 3 wells sampled up to 2x per year
- *Precipitation*: 1 rainfall sample per month x 2 stations (one in Canada, one in the US) x 12 months (monthly sample collection). Snow collection will not be necessary.
- *Streamflow*: 4 basins x 1 or 2 streamflow sample/basin/month (during ice-off) x 8 months of the year
- *Baseflow*: 1 ice-on streamflow sample/year in January or February x 4 basins

Summaries of sampling from 2022 to 2024 by type of survey, and 2020 to 2024 by basin are provided in Table 2 and Table 3, respectively. A graphical summary is provided in Figure 1.

Table 2. Summary of streamflow sampling undertaken from 2022 to 2024, separated by whether samples were taken as part of the UC-HAL longitudinal river surveys or as part of monthly river sampling (routine point sampling) at significant Water Survey of Canada (WSC) and United States Geological Survey (USGS) hydrometric stations: 11AA001, 11AA005, 11AA025, and 11AA031.

Survey type	No. of Locations	Collected By	2022		2023		2024	
			Per location	Total	Per location	Total	Per location	Total
Longitudinal River Surveys	21	UC-HAL	1-4	39	1-2	37	0-3	38
Routine Point Samples	4	WSC, USGS	0-5	14	0-8	18	5-13	36
TOTAL	25			53		55		74

Table 3. Summary of streamflow sampling undertaken from 2020 to 2024, separated into the four subbasin categories used in EMMA modelling, plus an additional category capturing tributaries and springs (as part of investigating additional source inputs) that are not part of the main stem Milk River. Counted samples include those taken from the corresponding WSC gauge in that area plus those in the same location category that were taken as part of the UC-HAL longitudinal river surveys.

Location Category	WSC ID	2020 Samples	2021 Samples	2022 Samples	2023 Samples	2024 Samples
North Fork Milk River (with St. Mary's diversion inputs)	11AA001	4	2	19	15	19
South Fork Milk River (natural headwaters)	11AA025	2	1	10	9	7
Main Stem Confluence at Milk River townsite	11AA005	1	2	9	10	12
Main Stem Downstream (East) of Confluence	11AA031	7	0	11	16	31
Tributaries and Springs	n/a	2	0	4	5	5
	TOTAL	16	5	53	55	74

Milk River Isotope Sampling Locations

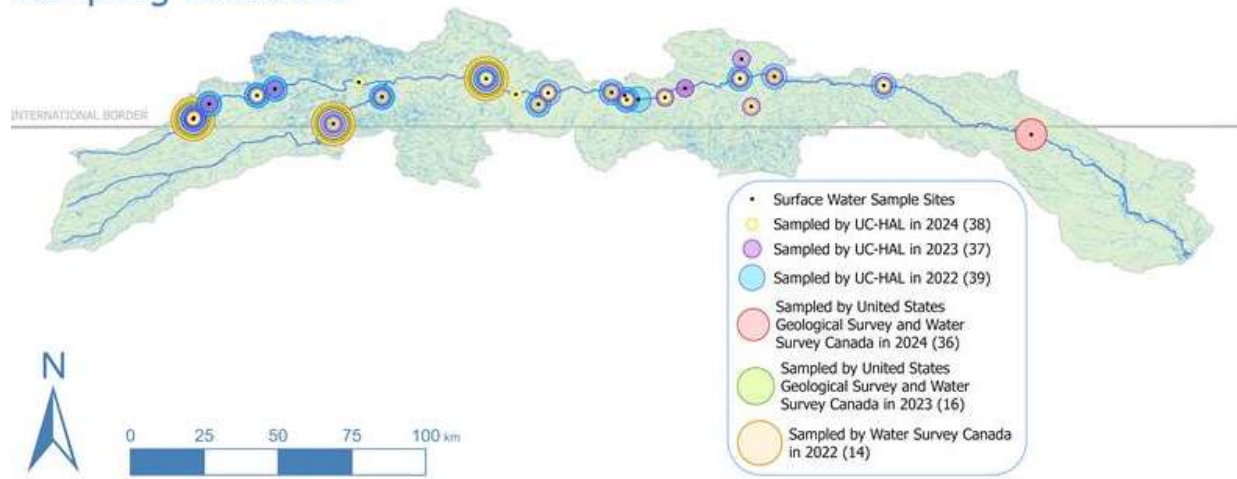


Figure 1. Map of streamflow isotope samples collected by UC-HAL, Water Survey of Canada and United States Geological Survey from 2022 to 2024, including frequency of sampling per location.

The University of Calgary Hydrologic Analysis Lab (UC-HAL) team performed longitudinal streamflow surveys collecting water samples at up to 21 sites per visit, depending on flows at the time of the survey. Mainstem sites were sampled more frequently with contributing tributaries being sampled when deemed necessary or feasible based on flow. Water Survey of Canada and the United States Geological Survey alternate sampling the four stationed hydrometric gauge sites, collecting point samples at the time of their visits. These point samples can be further subdivided into times of year when the collected isotope samples represent baseflow.

- Our fieldwork has spanned the portion of the Milk River watershed that falls within southern Alberta, from the North Milk River in the far west, all the way to where the mainstem Milk River trails southward across the Montana border. Our sampling sites account for the North Milk after the diversion canal, a short portion of the south fork of the Milk River ahead of its confluence with the North, and the mainstem Milk River flowing eastward. The south fork ahead of the confluence is notable as this reach is not influenced by the diversion at all.
- The sites that are located along the North Milk River and south fork are referred to in this report as the headwater region; everything downstream of the confluence is referred to as the mainstem Milk River.
- Our sampling regime also includes several sites that are located along tributaries to the Milk River; these include a possible groundwater spring located just downstream of Water Survey of Canada hydrometric station 11AA001 (North Milk Near Int Boundary), Red Creek, Breed Creek, and an unnamed site east of Breed Creek (informally called Fossil Creek).
 - Red Creek and the spring, MR004, are the two most consistently sampled sites; Breed Creek and so-called Fossil Creek have each only been sampled since 2023. Breed Creek appears to originate at the foot of the Sweetgrass Hills and may be of interest to sample in the spring or late winter; in the summer flows appeared to be low and it is unclear if this tributary can be considered connected to the Milk River throughout most of the summer and fall seasons, but it is an area of note as the topography in this region (near Aden) varies greatly and there are many ephemeral stream networks that may link to the mainstem Milk River.

A summary of the streamflow-isotope timeseries is provided in Figure 2.

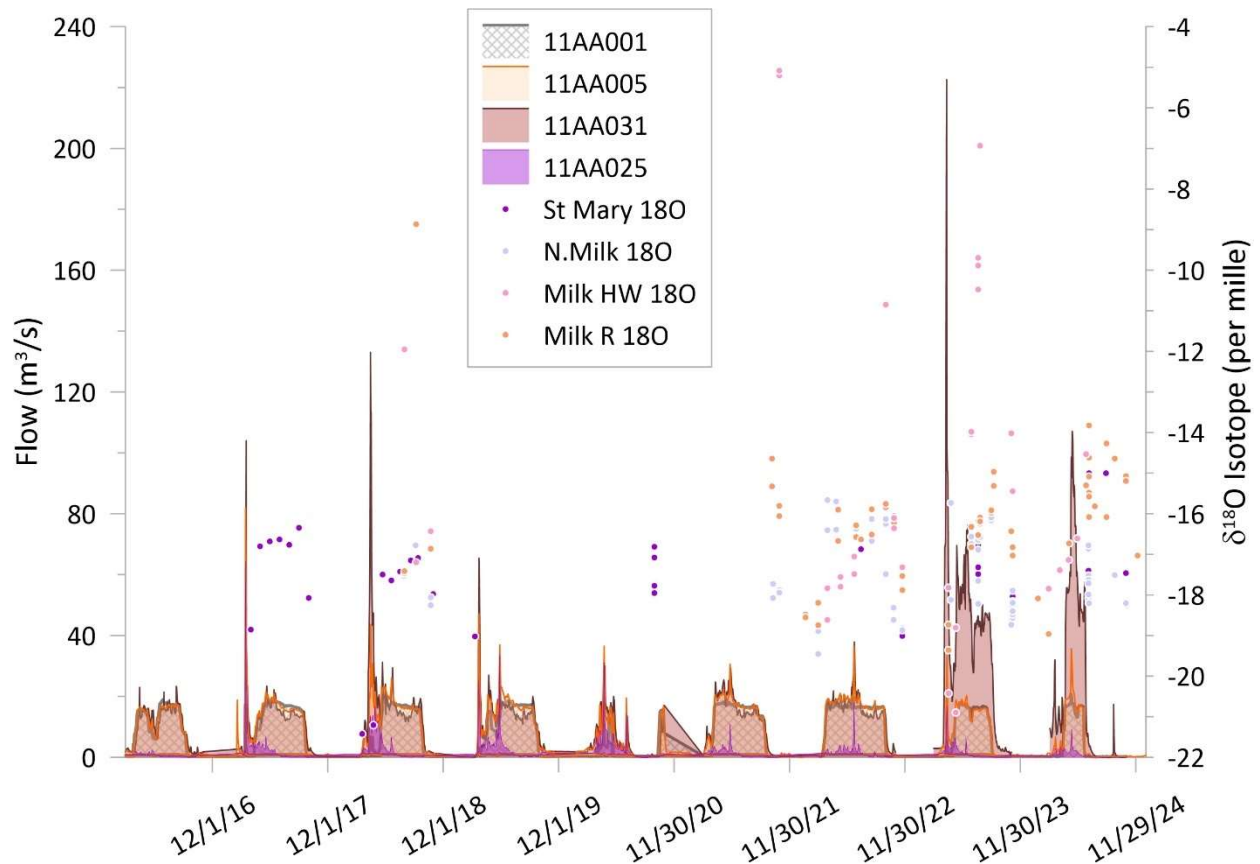


Figure 2. Streamflow-isotope timeseries from 2016-2024 developed from this IWI research.

Long-term Plan for Monitoring Network

Our research team is continuing to sample the primary gauge locations (11AA025, 11AA005, and 11AA031), and to work with WSC and USGS to retrieve samples they have collected as part of the National water isotope sampling network. These samples will be analysed at cost under the national monitoring program. We have also arranged an isotope in precipitation sampler to be installed and monitored by the Milk River Watershed Conservation Council (MRWCC) for longevity of the program and potential use of the isotope data for modelling.

2. Isotope & Hydrologic Modelling

2.1. Hydrometeorological Analysis

Average weather and climate data in the upper Milk River basin were required for calculating and estimating evapotranspiration proportions. Monthly climate data including average temperature, relative humidity, total evaporation, and total precipitation were downloaded from NCEP North American Regional Reanalysis (NARR) database. Gridded NARR data are spatially averaged within an 8-km buffers for each sub-basin. Meteorological variables retrieved from NARR are plotted at a daily resolution (January 2016 to December 2020) but

were aggregated to monthly data for use in the study (Figure 3). There were no significant differences in average monthly meteorological variables observed across the study period.

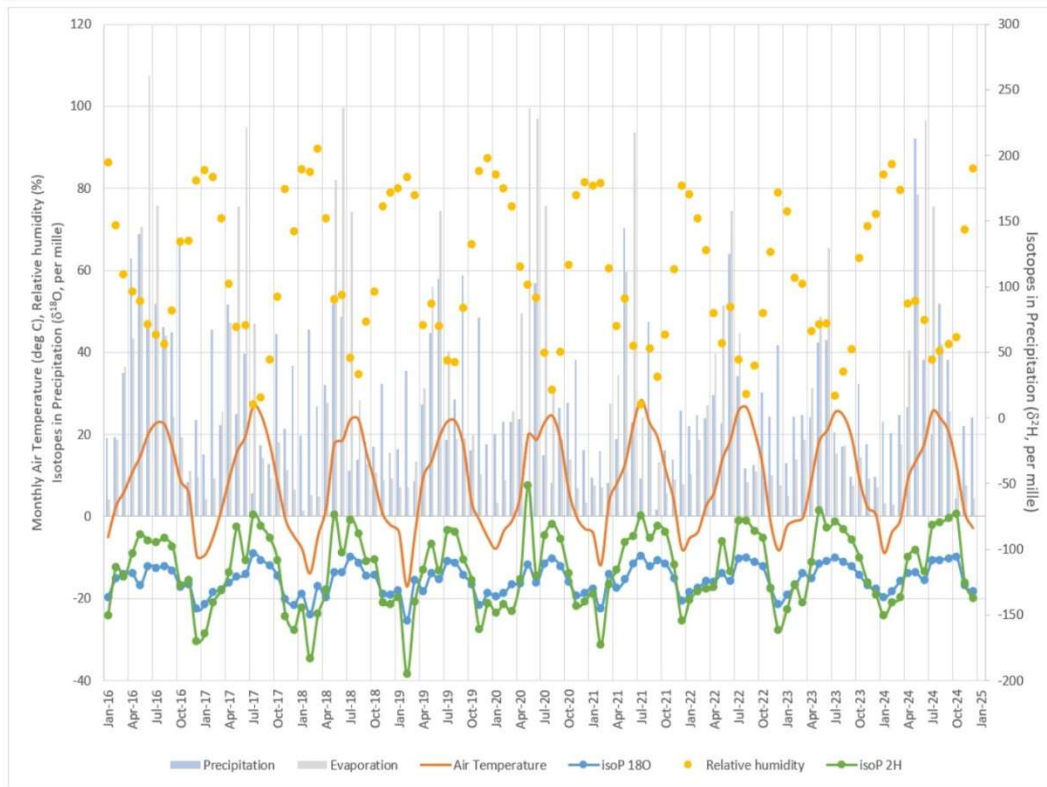


Figure 3. Summary of meteorological conditions obtained from NARR for the study period from January 2016 to December 2024, including modelled isotopes in precipitation signatures required for water balance modelling.

2.1.1. Isotope in Precipitation Forcing

Forcing data for the model were generated from the isotope in precipitation (isoP) model and were required for water balance modelling (Delavau et al. 2015). Modelled isotope concentrations were flux-weighted by the total precipitation for the point cells before averaging by the same method as the NARR data. IsoP uses observations from the long-term Canadian Network for Isotopes in precipitation (CNIP) and United States Network for Isotopes in Precipitation (USNIP), along with physiographic basin characteristics and meteorologic data from NARR. Time series (monthly) output from isoP is shown on Figure 3, and Figure 4 shows the variability in isotope in precipitation forcing across the Milk R basin, time averaged from 2016-2024. The more depleted precipitation composition at the headwaters in the most western portion, where the St. Mary River originates, and subsequently diversion inflows to the Milk River basin.

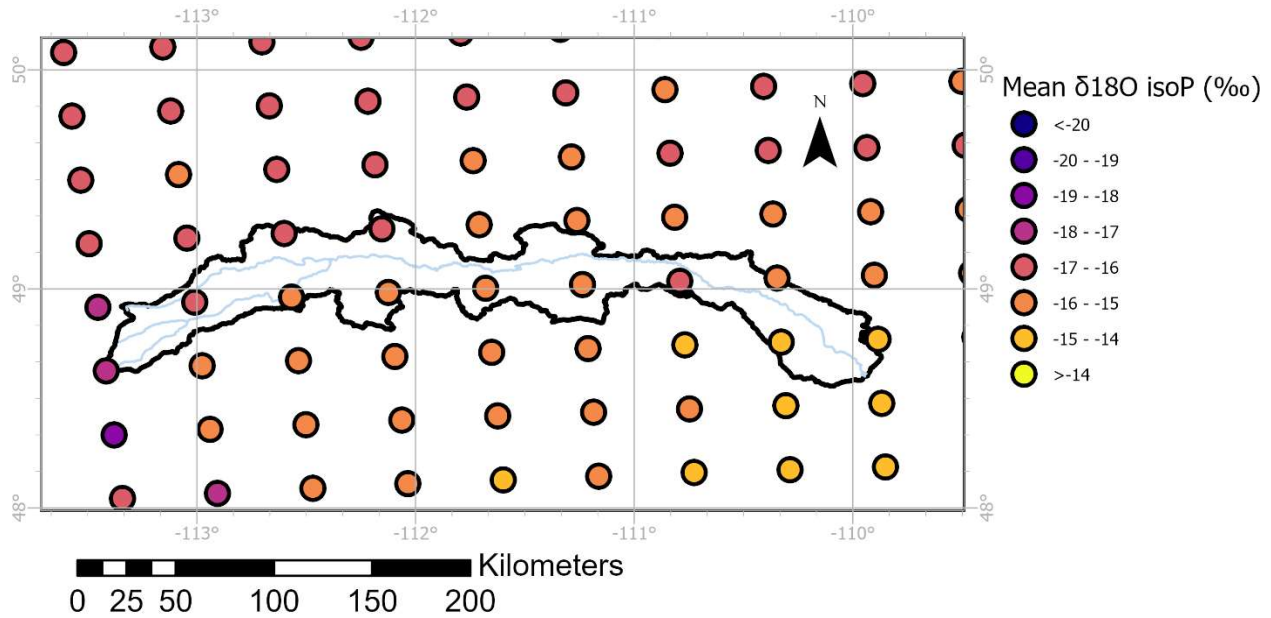


Figure 4. Spatial variability of the isotopes in precipitation input across the Milk River basin as predicted by iso P (2016-2024).

The monthly isotopic composition of precipitation was derived by the isoP model (see Section 2.1.1). Offset from the global meteoric water line (GMWL; $\delta^2H=8*\delta^{18}O+10$) was used as a measure of relative evaporative fractionation from one source or year to the next given the absence of observations of isotopes in precipitation to derive a true local meteoric water line (LMWL). A LMWL was estimated from isoP monthly modelled compositions (2016-2024) and found to be:

$$LMWL: \delta^2H = 7.21 \times \delta^{18}O - 3.57 \quad (1)$$

2.2. Landscape Analysis – Non-Contributing Areas

Prairie pothole or non-contributing areas of the SMM watershed were mapped as they are important for the modelling of the basin, and this work were integrated into the hydrological model to improve the estimation of regions (drainage area) dynamically contributing to runoff generation. Figure 5 presents the contributing area map for a 1 in 2-year rainfall event for the SMM basin.

Return Period = 2 years & Rainfall depth = 38.4 mm

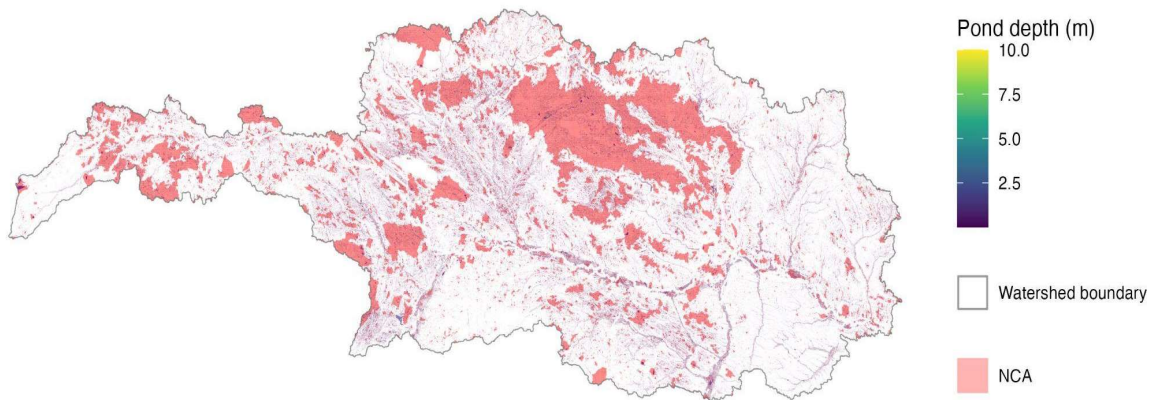


Figure 5. Map of prairie potholes with a 2-year return period; maps were generated for 2-, 5-, and 10-year return periods and are available for the SMM study region.

2.3. Hydrological Modelling

Under Annex 3 of the SMM UCalgary project, under the same MOU, an implementation of the HYPE hydrological model was developed for the SMM by PhD student Paul Coderre (supervisor: Al Pietroniro), and future water supply scenarios developed for the water resource management modelling. For consistency between Annex 2 and 3, the output from HYPE was used to drive the isotope tracer model output (MAITsim).

2.4. Model Agnostic Isotope Tracer (MAIT) Modelling

A model agnostic (i.e., can plug in with any hydrological model) isotope code is now complete and connected to a specific implementation of the HYPE model derived for Annex 3 of an IWI study, adding isotope simulation capabilities to HYPE (Holmes et al. 2024, <https://doi.org/10.5194/egusphere-egu24-12870>). The MAITsim (Model-Agnostic Isotope Tracer simulation) code has been developed in R (available on GitHub: <https://github.com/tegan-holmes/MAITsim>) and is a post-processor for isotope simulation. As a proof-of-concept, this modelling tool was applied to the Milk River portion of the HYPE hydrological model setup from Annex 3 (Section 2.3).

The MAITsim simulations are linked to the HYPE model described above and therefore share its strengths and limitations. The model simulation period of HYPE was extended only to 2018, therefore paired simulation-observation error comparisons was only partially feasible (overlapping with isotope data).

2.4.1. Model Setup Methods

MAITsim was run on water-balance output from Paul's HYPE model (both ^{18}O and ^2H) using daily simulation from 1970 to 2018, with spin up from 1970 to 1980. NARR and isoP were used as atmospheric forcing input for MAITsim. HYPE simulates naturalized flows (no

diversion etc.), while isotope observations are often diversion affected, therefore results are only shared for non-diversion headwater (11AA025) here as a proof-of-concept for the model. Isotope observations are available from 2017 to 2024, which has only a partial overlap with the HYPE simulation, results use a period of the same length from the HYPE simulation (2011 to 2018).

The HYPE model has up to 7 water-balance storages per sub-basin, with shallow groundwater (i.e., baseflow) assumed to be analogous to ‘Soil layer 3’ and river water to the ‘Main river’ (Figure 6).

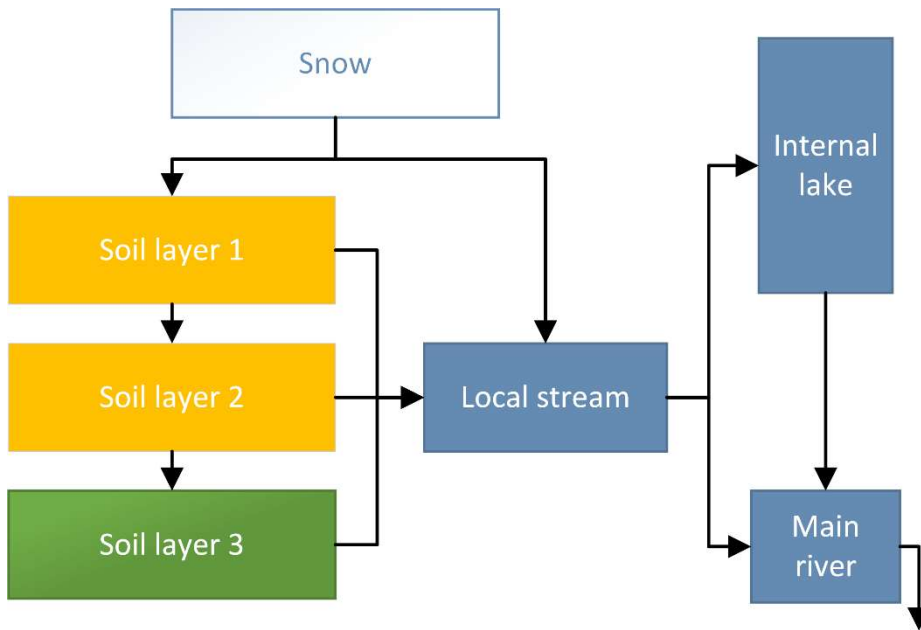


Figure 6. HYPE model storages for a single sub-basin, with the ‘baseflow’ source highlighted in green

2.4.2. MAITsim Model Results

The modelled HYPE-MAITsim isotope-isotope framework relative to observations at 11AA025 suggests that evaporation (volumetric loss) agrees with observations because the simulations produce the same LML slope and range of isotopic values (Figure 7). The simulation does not have the same ‘depleted’ range as observations (no simulated values in the ‘snow’ range of the isotope-isotope framework).

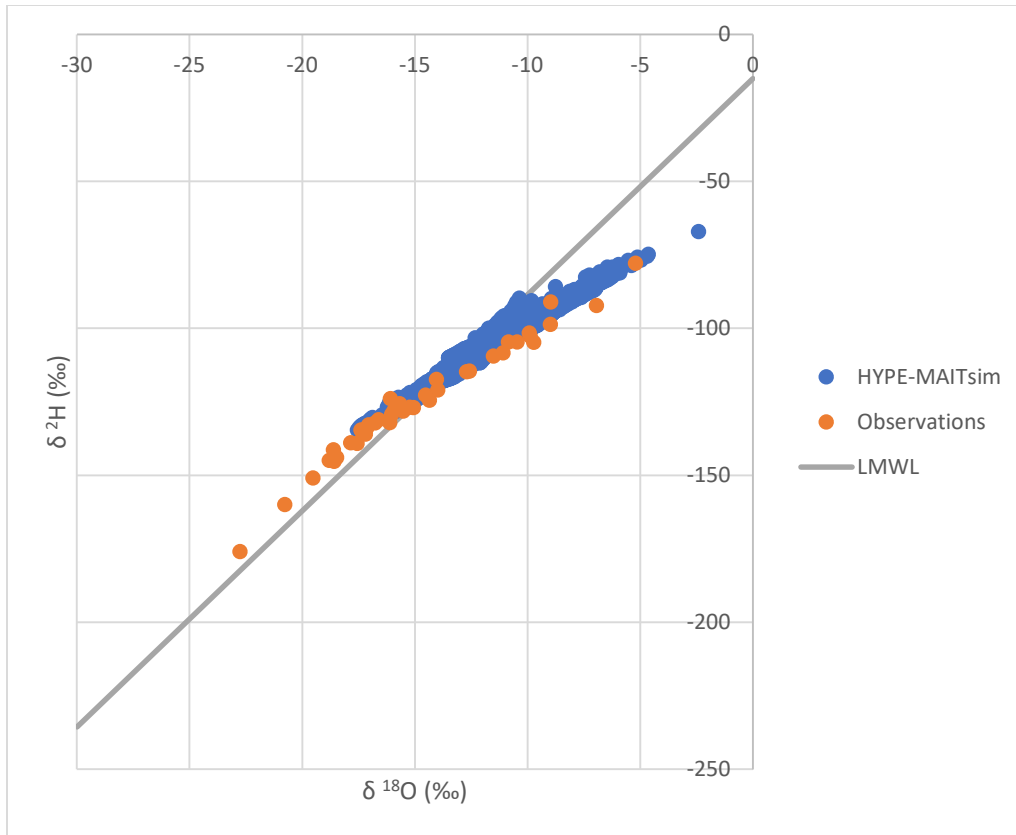


Figure 7. Isotope-isotope framework comparing HYPE-MAITsim simulated evaporatively enriched values relative to observed isotope observations collected during the simulation period (2016-2018).

Streamflow hydrographs and isographs at 11AA025 comparing observed and HYPE-MAITsim simulated values are presented on Figure 8. HYPE model flows are reasonable representations of observed gauge flow with statistics indicating under-estimation of peak flow, but reasonable timing and normal/low flows (Figure 8a). Isotope simulation is reasonable for the limited overlap period in summer but does not exhibit the observed cold/old water signal seen in the isotope observations (Figure 8b).

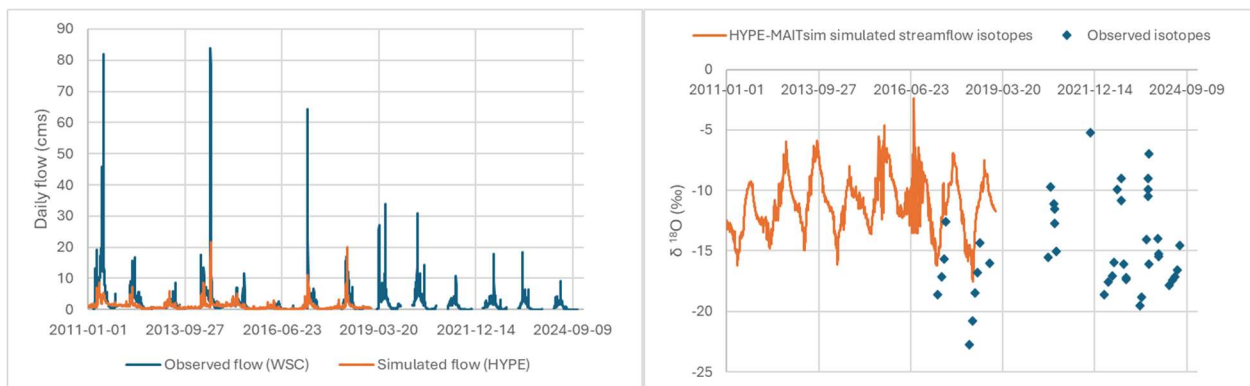


Figure 8. Observed and simulated (a) hydrographs and (b) isographs at 11AA025.

Due to the limited overlap of the timeseries of simulations and observations, daily average annual hydrographs and isographs were generated (Figure 9). These demonstrate that late summer is well simulated overall for total flow, isotope composition, and evaporative enrichment. Late fall, winter and early spring have limited isotope data, but what data there is points to incorrect HYPE source modeling: total flow is reasonable, but streamflow is more enriched than observed. These flows should be sourced from a minimally enriched storage or from snowmelt and they are not. Wet season (spring and early summer) is not well simulated, overall. Total flow is often too low, and isotopes are too enriched (should be old unenriched water, snowmelt or rain, not evaporated water).

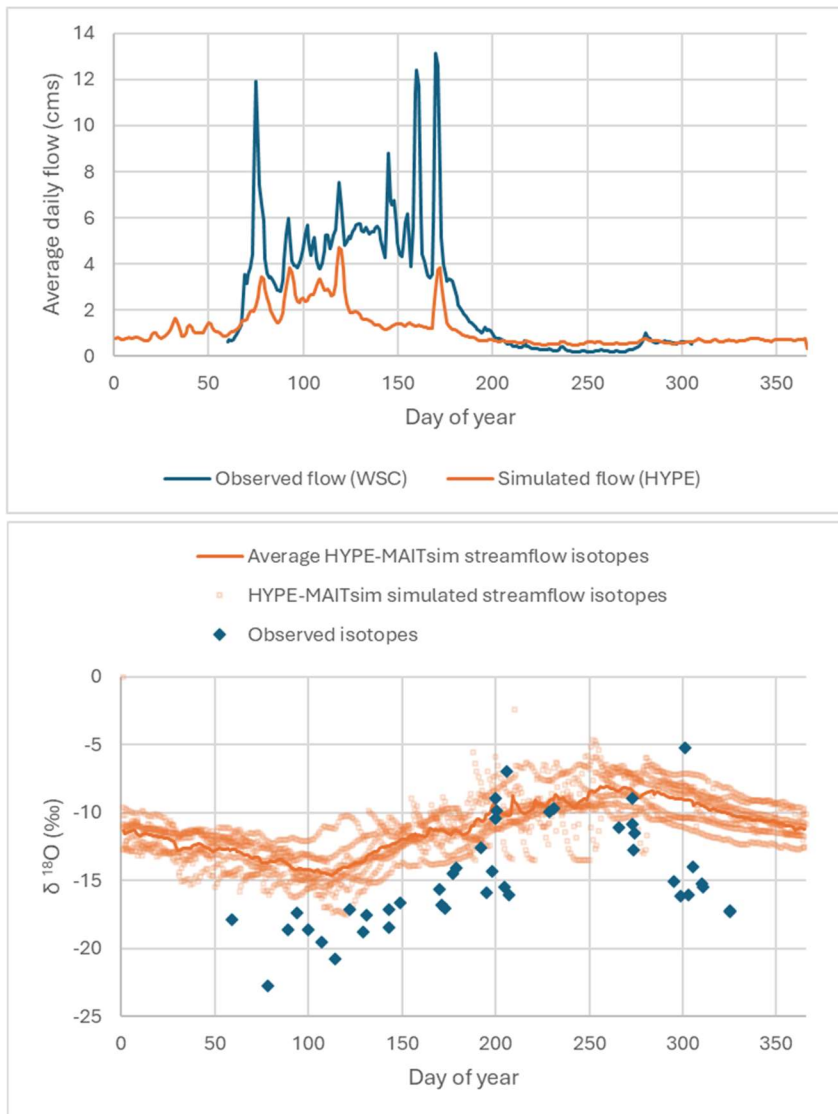


Figure 9. Daily average annual hydrographs (top) and isographs (bottom) for the Milk River headwaters (11AA025).

2.5. Fully Coupled Isotope-Hydrological Modelling

As a proof-of-concept, the isoWATFLOOD physically based coupled isotope-hydrological model was setup using the model agnostic framework (MAF) for the Milk River basin. First generation coupled isotope- hydrological simulations were completed in 2023 in a fusion of HYPE and CHARM (WATFLOOD). The isotope code from isoWATFLOOD was merged with HYPE subbasin structure and resulted in:

- Development of a functioning HYPE-CHARM fusion model with 1st generation isotope simulations
- Data files (sub-basins, HRU, precipitation, temperature) from HYPE model (direct from Paul Coderre’s model, another SMM project)
- CHARM regroups HRU into GRU, and uses its own parameters and process models, including the embedded isotope model isoWATFLOOD
- Isotope specific input files (initialization and isotopes-in-precipitation) have been created, allowing the simulation of isotopes in all fluxes and storages for the Milk River fusion model
- The model can also link to isotope observation files for streamflow, allowing for automated isotope-enabled calibration of the model
- Fusion model is organized on a sub-basin structure, not gridded like the previous iteration (fewer simulation units, with a hydrologically coherent organization)
- The current model includes the upper Milk River, up to the Fresno Reservoir. Scope based on the location of isotope sampling: mostly Canada and some near border.

As the isoWATFLOOD-HYPE model relies on input files from the HYPE model (see Section 2.3), the simulation period currently ends in 2015. A framework with the observed streamflow and simulated results (Figure 10) shows the inadequacy of the default parameters of this isoWATFLOOD-HYPE fusion model: evaporation and old water contributions are modeled inaccurately (Figure 10).

- Some observed isotope samples come from much lower on the LMWL than any on the simulated set, so the model does not include enough saved snowmelt/unevaporated groundwater.

- Evaporation is somewhat too low (simulated LML has a higher slope than the observed LML), summer evaporation needs to increase.

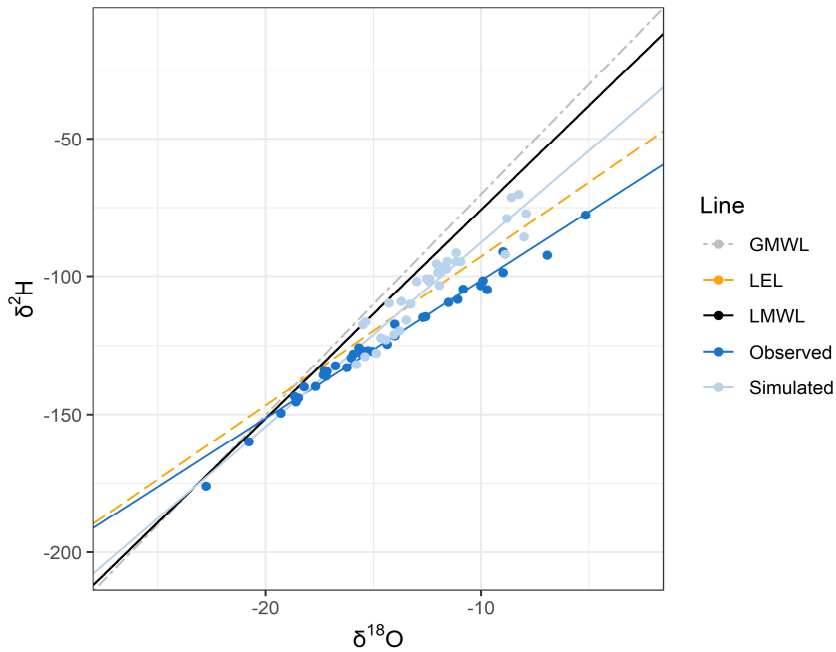


Figure 10. Simulated relative to observed isotope framework for the Milk River basin at AB11AA0280 (no diversion included in the model), derived by HYPE-CHARM fusion model (uncalibrated).

To improve the model, a multi-objective optimization using both streamflow and isotopes would need to be performed, including evaluation of hydrological processes and storages (e.g., evaporation, soil moisture) against

benchmark data (e.g., GLEAM). This would facilitate an ensemble analysis on the contribution of groundwater to streamflow as we move through the basin, as well as more accurate partitioning of diversion inflows as a proportion of total flow at each gauge. This work was beyond the scope of the current project; a subsequent proposal was submitted early in 2024 to continue a minimal investment in the isotope monitoring network and to advance the coupled isotope-hydrological modelling using multiple hydrological models (HYPE, MESH and SUMMA) and for parameter optimization, including potholes and diversion v. natural scenarios, to the IWI Study Board.

3. Source Separation

Analytical water balance modelling was used to identify distinct sources or end-member components of streamflow contributing in the SMM, and their relative contributions to the Milk River total flow.

3.1. Isotope Framework

A long-term isotope framework was generated using all isotope samples retrieved from the 2020 survey, historical isotope data (Annex 1), and the established monitoring network from 2022-2024 (Annex 2). This was important as a first step in characterizing the isotopic “endmembers” for the system, including limiting enrichment (star) and evaporative fractionation (cross) (Figure 11). Frameworks were also plotted by riverine system (Figure 12a) and for the Milk River only, by inter-annual variation (Figure 12b).

Isotope mass balance theory is based on earlier efforts in Canada derived from Gibson et al (2021). The equilibrium fractionation factor (α^*) was computed using both ^{18}O and ^2H and the temperature data (Horita et al. 2008), which gave the equilibrium factor, ε^* . The kinetic fractionation (ε_k) was similarly computed using experimental derived kinetic diffusivities for ^{18}O and ^2H and the relative humidity data (Horita et al., 2008). The isotopic composition of water vapour (δ_A) was assumed to be in equilibrium with precipitation, flux-weighted by monthly precipitation. All monthly δ_P , δ_A , ε^* , ε_k , and α^* values were averaged annually by water year (October to September) and averaged by sub-basin. Evaporative fractionation of isotopes was estimated using the Craig & Gordon model (1965) via the end point δ_E (per mille):

$$\delta_E = \frac{\left(\frac{\delta_P - \varepsilon^*}{\alpha^*}\right) - h\delta_A - \varepsilon_k}{1 - h - \varepsilon_k} \quad (2)$$

Where h is relative humidity averaged over the period of calculation, δ_A is the atmospheric composition assumed to be in equilibrium with precipitation ($\delta_A = (\delta_P - \varepsilon^*)/\alpha^*$). For precipitation, points were either amount weighted (by amount of precipitation) or evaporation flux-weighted (to account for seasonal changes in the amount of evaporation), according to Equation (4). δ_P was amount weighted by the precipitation flux (P), and δ_E by the evaporation flux (E), for n months (years) of data:

$$\delta_{seasonal} = \frac{\sum_{i=1}^n flux_i \times \delta_{flux_i}}{\sum_{i=1}^n flux_i} \quad (3)$$

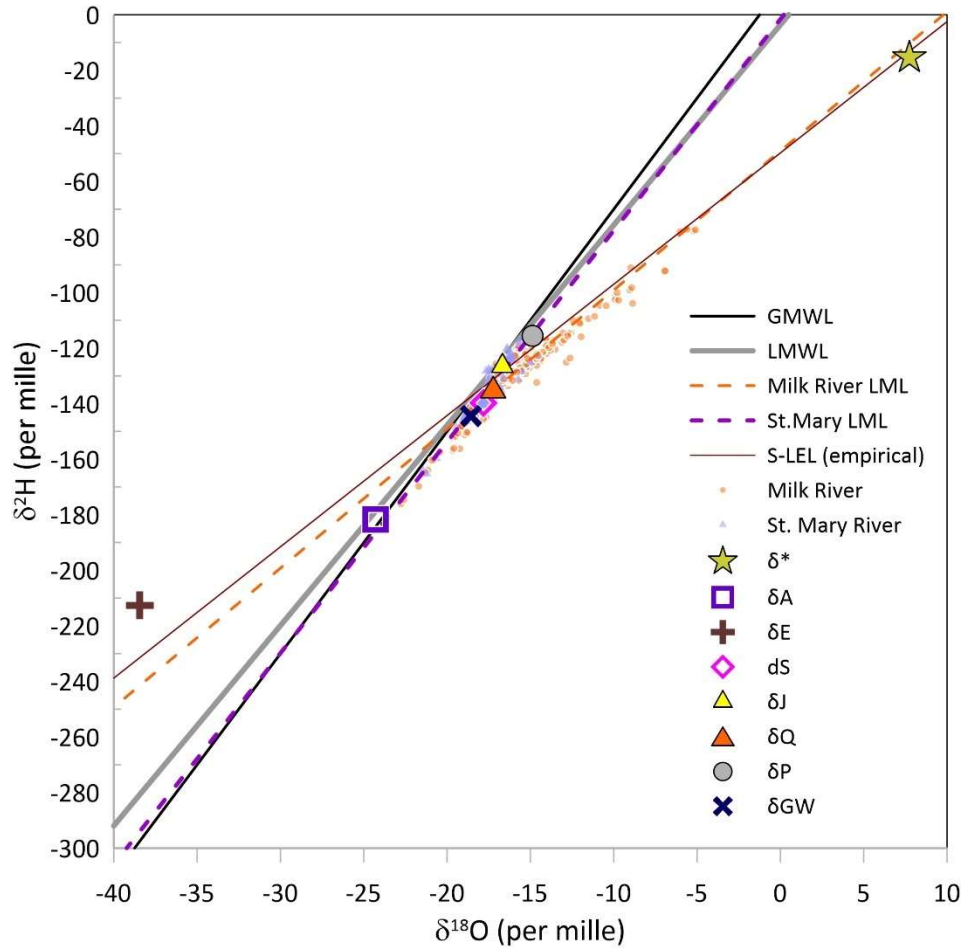


Figure 11. Long-term isotope framework developed from all samples (2016-2024) with flux-weighted end points. End points provided in Table 4.

Table 4. End points from long-term framework derived from samples collected 2016-2024, by river basin.

End Point	Description	Milk		St. Mary	
		$\delta^{18}\text{O}$ (‰)	$\delta^2\text{H}$ (‰)	$\delta^{18}\text{O}$ (‰)	$\delta^2\text{H}$ (‰)
δ^*	Limiting enrichment	7.73	-15.36	3.15	-36.4
δ_S	Steady-state composition ($I=Q$)	-17.8	-139.7	-16.0	-120.9
δ_P	Amount-weighted precipitation	-15.3	-117.9	-15.9	-122.5
δ_A	Atmospheric composition	-24.3	-181.7	-24.3	-182.1
δ_E	Amount-weighted vapour loss	-43.9	-243.5	-43.3	-234.8
δ_Q	Amount-weighted streamflow	-17.2	-134.1	-15.9	-120.9
δ_J	Amount-weighted basin inflow	-16.7	-124.0	-	-

Samples were categorized and regressed (into local mixing lines, LML) by year, river, and source (duplicates were removed but tested for quality control). Frameworks plotted $\delta^{18}\text{O}$ (‰) against $\delta^2\text{H}$ (‰), with different symbols used for different categories of samples (by year, river or source). Equations representing the line of best fit were produced for each

category and the R^2 reported for each regression line (Table 5). A minimum of four samples was required for a regression to be conducted.

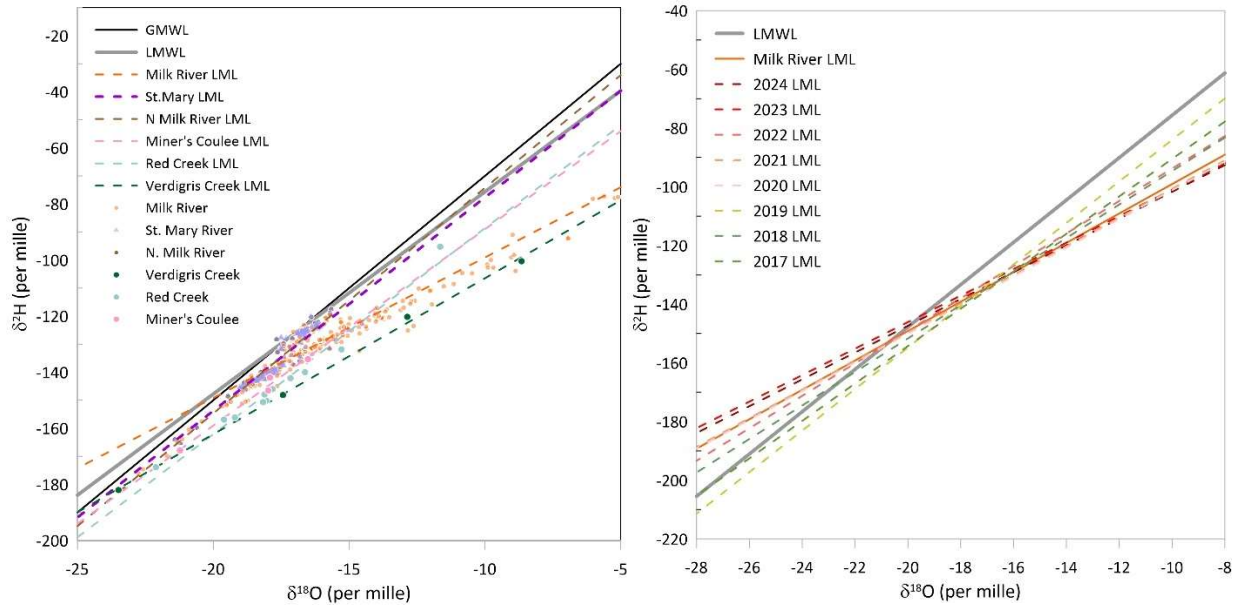


Figure 12. Isotope framework by (a) river or tributary input, and (b) for the Milk River basin only by year. Note axis scale differences.

Table 5. Local mixing line (LML) equation of best fit (linear) by river in the SMM, where $Y = \delta^2H$ and $X = \delta^{18}O$ based on period stated

River	Time Period	LML Equation	R^2
North Milk R	2016-2019	$Y = 8.040X + 6.132$	
Miner's Coulee	2016-2019	$Y = 6.998X - 19.06$	
Red Creek	2016-2019	$Y = 7.346X - 15.19$	
Verdigris Creek	2016-2019	$Y = 5.561X - 50.89$	
St. Mary R	2016-2024	$Y = 7.6073X - 1.5998$	0.8613
Milk R	2016-2024	$Y = 5.0072X - 49.016$	0.8989
Milk R	2017	$Y = 6.3751X - 26.774$	0.8903
Milk R	2018	$Y = 5.0742X - 37.603$	0.8828
Milk R	2019	$Y = 7.0736X - 13.296$	0.9992
Milk R	2020	$Y = 4.8873X - 52.303$	0.8801
Milk R	2021	$Y = 4.8828X - 51.898$	0.9964
Milk R	2022	$Y = 5.5298X - 38.497$	0.8639
Milk R	2023	$Y = 4.5141X - 55.831$	0.8873
Milk R	2024	$Y = 4.5648X - 56.064$	0.9197

End points for the isotope framework, such as the desiccation point, or limiting enrichment (δ^*) and input composition (δ_i) in per mille (‰) were computed from water and isotope mass balance equations, as reported by Gibson (2002):

$$\delta^* = \frac{h\delta_A + \varepsilon_k + \frac{\varepsilon^*}{\alpha^*}}{h - 10^{-3} \cdot \left(\varepsilon_k + \frac{\varepsilon^*}{\alpha^*}\right)} \quad (4)$$

Relative to the desiccation point, the isotopic and water balance steady state (δ_s) composition is defined as

$$\delta_s = \frac{(\delta_l + mx\delta^*)}{(1 + mx)} \quad (5)$$

Where x is the E/I ratio defined by Equation (14), and $m = (h - \varepsilon^*/1000)/(1 - h + \varepsilon_k/1000)$, which represents the slope of the $\delta^{18}\text{O}$ to $\delta^2\text{H}$ fractionation line, as defined by Allison et al., (1983) and Welhan & Fritz (1977). Figure 13 presents the δ^* and δ_s for the SMM relative to the LML from riverine isotope samples in the St. Mary and Milk rivers. The heightened evaporative loss in the Milk River system by the lower slope of the Milk River LML (orange dashed) relative to the St. Mary (dashed purple) which tracks the long-term average of flux-weighted precipitation (blue solid).

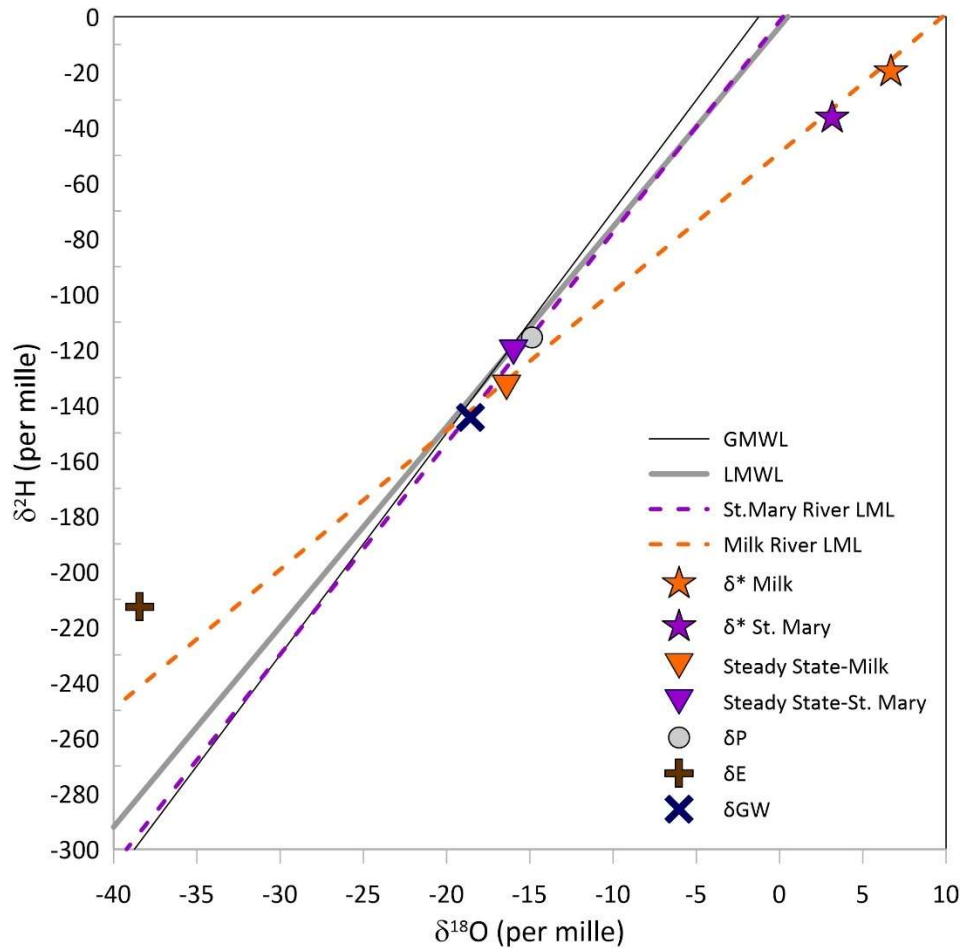


Figure 13. St. Mary and Milk River local mixing lines (2017-2024) relative to limiting enrichment (δ^*) and steady state isotopic composition (δ_s) for the Milk (orange) and St. Mary (purple) rivers.

The slope of deviation of samples from the meteoric water line due to evaporation is caused by evaporation flux, with the upper limit of this slope defined as the local evaporation line

(LEL). There are several methods used to estimate this slope, including the analytical equation that measures the offset of ^2H from ^{18}O (Equation (6)):

$$S_{LEL} = \frac{\left[\frac{h(\delta_A - \delta_P) + (1 + \delta_P)(\varepsilon_K + \varepsilon^+/\alpha^+)}{h - \varepsilon_K - \varepsilon^+/\alpha^+} \right]_2}{\left[\frac{h(\delta_A - \delta_P) + (1 + \delta_P)(\varepsilon_K + \varepsilon^+/\alpha^+)}{h - \varepsilon_K - \varepsilon^+/\alpha^+} \right]_{18}} \quad (6)$$

Where the numerator is computed using the ^2H isotope, and denominator the ^{18}O isotope. Additionally, S_{LEL} can be derived empirically using observations, connecting the limiting enrichment point (δ^*) and either the (a) evaporative endpoint (δ_E), (b) steady state composition (δ_S), (c) flux-weighted long-term average whole basin inflow (δ_Q), or the (d) flux-weighted precipitation (δ_P), or (e) groundwater, representing the long-term flux-weighted average of precipitation (δ_{GW}) linearly to estimate the S_{LEL} . Estimation of the S_{LEL} via these different methods is presented in Table 6.

Table 6. Comparison of estimated S_{LEL} based on different methods and end points.

Method	S_{LEL}	Intercept
Analytical: Equation (6)	7.593	-
Empirical: δ_E to δ^*	4.364	-45.57
Empirical: δ_S to δ^*	4.933	-51.43
Empirical: δ_Q to δ^*	4.848	-50.56
Empirical: δ_P to δ^*	4.583	-47.82
Empirical: δ_{GW} to δ^*	4.905	-53.30

3.2. EMMA Modelling

One of the fundamental questions to be addressed in this study is if isotopes can be used to estimate the amount of diverted streamflow (St. Mary diversion, 11AA001) entering the Milk River system as a proportion of the downstream Milk River flows (i.e., 11AA005 and 11AA031). End-member mixing analysis (EMMA) is an analytical tool used to perform two-component isotope hydrograph separations (IHS) along a mixing line defined between distinct end points, determining the relative contribution of those two end points to a total or mixed isotopic sample. Following from a simple flow balance, we can derive the EMMA model:

$$Q_T = Q_1 + Q_2 \quad (7)$$

$$\delta_T Q_T = \delta_1 Q_1 + \delta_2 Q_2 \quad (8)$$

Where Q_1 , Q_2 are the volume flow contributions (m^3/s) combining to Q_T . Similarly, δ_1 , δ_2 are the source water isotopic compositions, required to be sufficiently distinct and the only

components contributing to the total mixed isotopic composition, δ_T . If we define f_1 as the fraction of total streamflow contributing from source 1 (Q_1/Q_T), and similarly f_2 as Q_2/Q_T , where f_1 and f_2 sum to 1, then Equation 13 can be solved for the total isotopic composition:

$$\delta_T = f_1\delta_1 + (1 - f_2)\delta_2 \quad (9)$$

Where it then follows that the contributions from source 1 and source 2 can be estimated using isotopic methods alone:

$$f_1 = \frac{\delta_T - \delta_2}{\delta_1 - \delta_2} \quad \text{and} \quad f_2 = 1 - f_1 \quad (10)$$

Fractional source contributions are reported in per cent by multiplying by 100. The EMMA is applied to each isotope individually; error in the fractional component estimations was based on the percent deviation of source contributions from one another:

$$Error (\%) = \frac{f_{18O} - f_{2H}}{f_{2H}} \quad (11)$$

Daily discharge data were retrieved from Water Survey of Canada's (WSC) HYDAT database through the Environment Canada Data Explorer for Stations 11AA001, 11AA025, 11AA005, and 11AA031 between 2016 and 2020. Daily flow measurements are seasonal and available from March to October, except for Station 11AA005 which has measurements for the entire year. To keep time-dependent averages consistent, only the March to October data was used from Station 11AA005. WSC gauges used, and their drainage areas and mean annual discharge from 2016 to 2020 are included in Table 7. Gauge 11AA025 is distinctive in that it is a headwater gauge for the Milk River and unaffected by the diversion. Gauge 11AA001 represents the St. Mary River inflows to the Milk River, and 11AA005 is downstream of the confluence of the headwater and diversion inflow location, representing a first mixing point. Furthest downstream is 11AA031 at the eastern crossing before the Milk River re-enters the United States, representing the longest flow path for the Milk River in Canada.

Table 7. Gauges where EMMA was performed; basin IDs correspond to those delineated on Figure 1. *Gauges where natural flows are estimated for the treaty.

Basin ID	WSC ID	Name	Subbasin Area (km ²)	Mean Annual Discharge 2017-2024* (m ³ /s)	Mean Annual Discharge (entire record) (m ³ /s)
1	11AA025 [^]	Milk River at Western Crossing of International Boundary	1054	2.05	12.1
2	11AA001 [^]	North Milk River near International Boundary	239	9.33	10.0
3	11AA005	Milk River at the town of Milk River	1440	8.00	8.86
4	11AA031 ^{^^}	Milk River at Eastern Crossing of International Boundary	3793	11.02	14.5

*2024 WSC data were provisional.

[^]Seasonal gauge operational from 01-Mar to 31-October (±2 days in any given year) from 1909 to present, except 11AA025 which became operational in 1937.

^{^^}Record available seasonally (01-Mar to 31-Oct) from 1909-2022; no data from WSC gauge 2023 or 2024, but USGS gauge just downstream used as substitute.

3.2.1. Groundwater (Baseflow) Analysis

EMMA was first applied to perform a streamwise assessment of groundwater contribution to the Milk River, beginning with the headwater (non-diversion impacted; 11AA025), and ending at the eastern crossing (11AA031). Because the isotopic composition of groundwater is close to that of the diversion-affected flow, groundwater estimation for just 2020/2024 (no diversion) was done as a control.

Results should be interpreted with caution as the sample size (n) for 2020/2024 is smaller and represents a limited period (Sept-Nov) and samples. In the headwater basin (11AA025), groundwater contributes 28% on average, of total streamflow annually, which decreases in the streamwise direction to 10% on average of total annual streamflow (11AA031) (Figure 14).

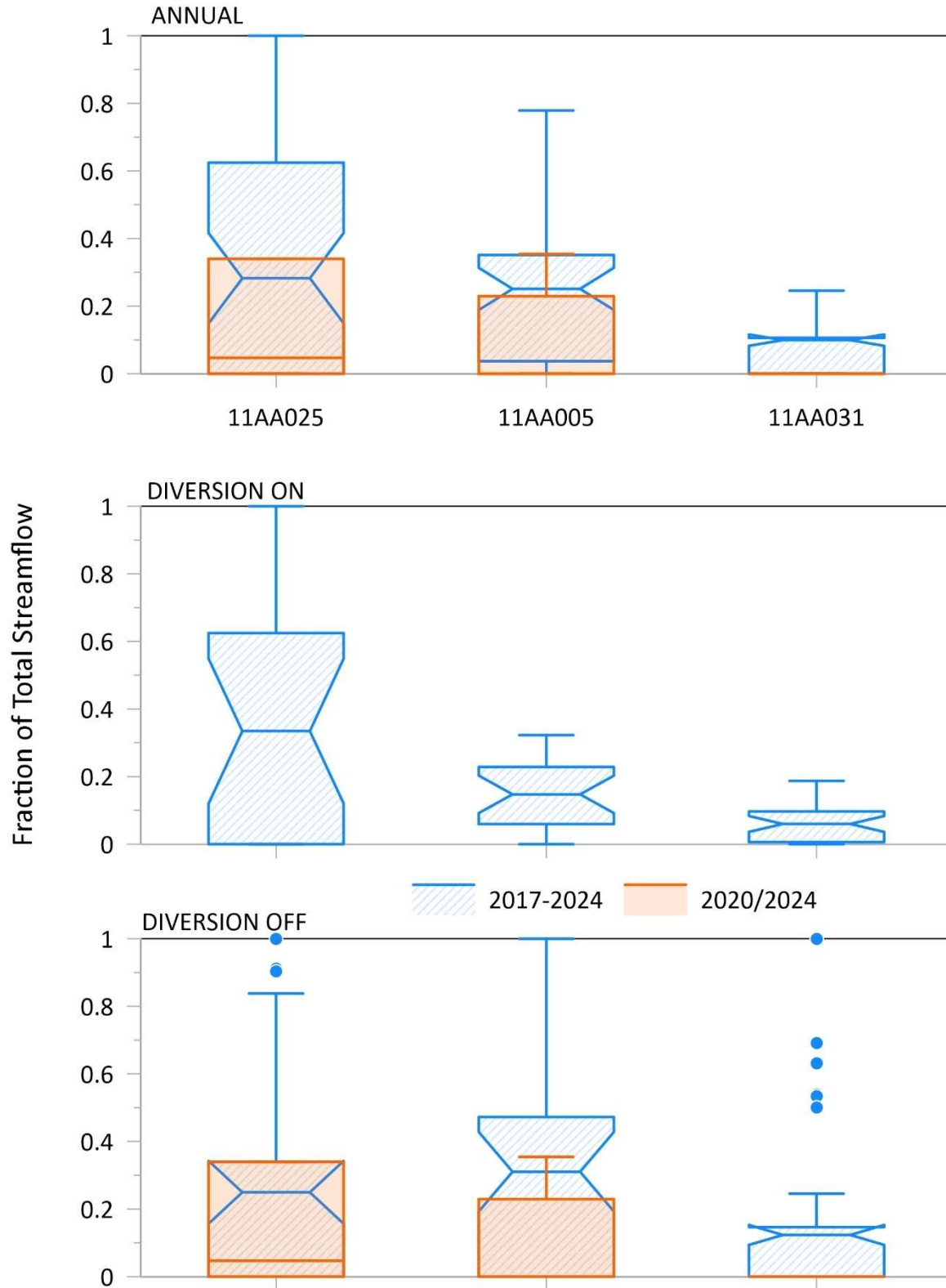


Figure 14. Groundwater (baseflow) separation using EMMA approach in streamwise direction from all samples (2018-2023) relative to 2020 (no diversion); 2020 included only two samples from end of September and early October. IQR boxes are 25/75 with median value, whiskers are 10/90 with outliers at 1.5xIQR.

Groundwater contributions are highest and most variable in the upstream headwaters. During non-diversion season (diversion off), groundwater contributions are about the same in the headwater (as they should be given the diversion has no impact there), but rise slightly to 31% and 12%, on average, for the mid (11AA005) and downstream (11AA031) reaches. Lower groundwater contributions are detected during the diversion seasons for mid and downstream reaches, which is contrary to the headwater basin (11AA025) behaviour which sees an increase to 33% on average groundwater contribution.

The physically based HYPE model also simulated baseflow fraction, using lowest soil layer as baseflow source (2011 to 2018), and was compared relative to the EMMA separations (Figure 15). HYPE baseflow represented a higher fraction of total streamflow than the isotope separations predict, however were within the range predicted by the isotopes (Figure 16).

Figure 15. Daily average annual timeseries separation of HYPE simulated baseflow relative to total flow.

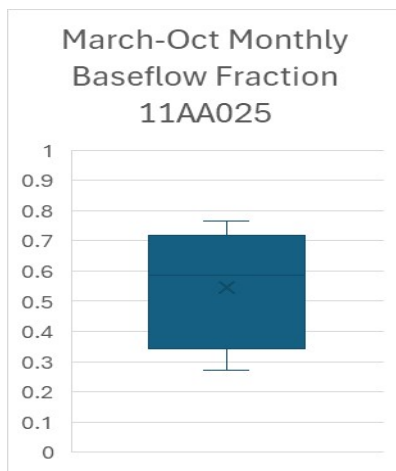
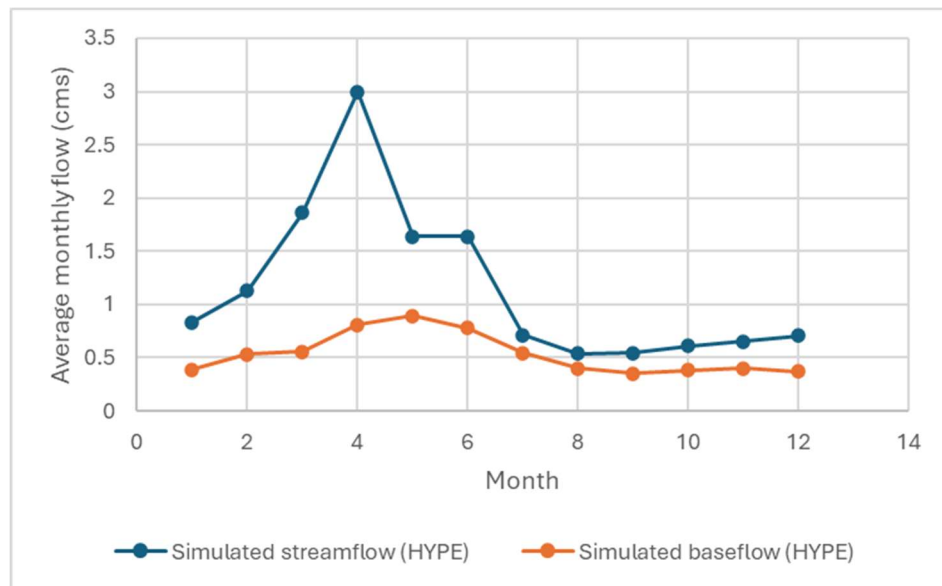


Figure 16. HYPE simulated baseflow fraction from March to October for the entire period of simulation for the headwater basin, 11AA025.

Daily simulated baseflow splits ranged from 0 to 100% baseflow due to the long-term simulation, demonstrating a high range of variability in the model. The long-term (multi-year) average baseflow contribution for March-October is 49% of total flow (with higher baseflow contribution months generally having lower total flows), compared to 33% predicted by the sporadic isotope observations (non-continuous sampling in time).

Average HYPE-MAITsim soil and groundwater simulations relative to precipitation input and average observed groundwater composition are plotted to further assess the groundwater partition (Figure 17). Ideally, groundwater is close to the long-term average of precipitation input, or at least close. Here simulated soil and groundwater compositions are stable, which is reasonable, however, simulated groundwater is more enriched than most precipitation (which it wouldn't be in reality) and much more enriched than observed groundwater.

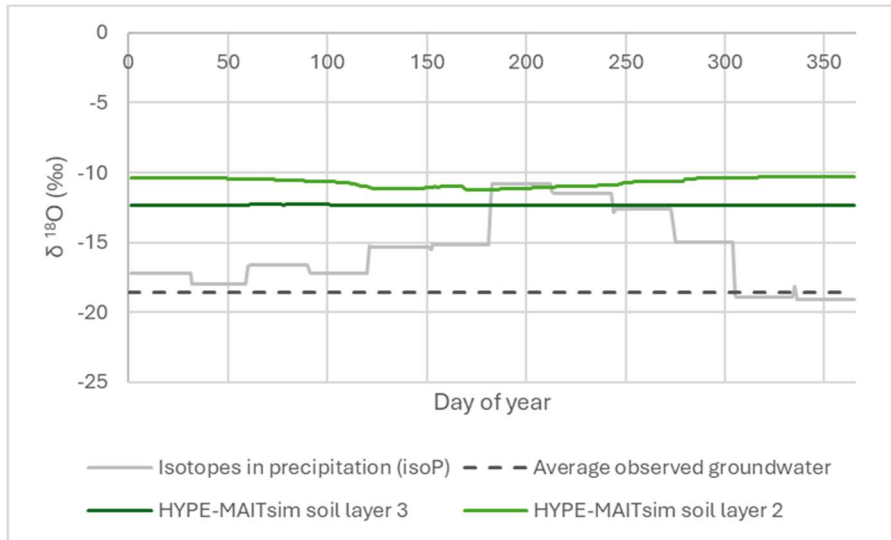


Figure 17. Groundwater simulated and observed relative to precipitation input.

3.2.2. Diversion Inflow Analysis

EMMA was also applied to estimate the relative contribution of diversion water to total streamflow in the streamwise direction. For this analysis, dominant end members for the mixing model were identified (Figure 18) and are summarized in Table 8.

Table 8. Summary of EMMA endmembers identified in the study using data from 2016-2024, corresponding to Figure 18.

EMMA End Pt	Gauge, Location	Description	δ ¹⁸ O	δ ² H
1	11AA001	Diversion inflow to the Milk (2017-2024)	-15.99	-121.0
	11AA025	Milk – upstream headwater (2017-2023)	-16.25	-132.2
	11AA005	Milk – downstream of confluence (2017-2024)	-16.67	-128.7
	11AA031	Milk – Eastern crossing	-15.31	-124.4
	GW wells	Groundwater samples	-18.57	-144.4
2	isoP	Flux-weighted precipitation (2017-2024)	-14.66	-113.4
3	δQ (2021)	Maximum headwater enrichment	-5.15	-77.7
	11AA005	Milk – at town site, Diversion season	-16.18	-125.1
	11AA025	Milk – headwater, Diversion season	-15.88	-125.0
	11AA001	St Mary inflow, Diversion season	-16.99	-129.2
	11AA031	Milk - Eastern crossing, diversion season	-16.14	-125.2

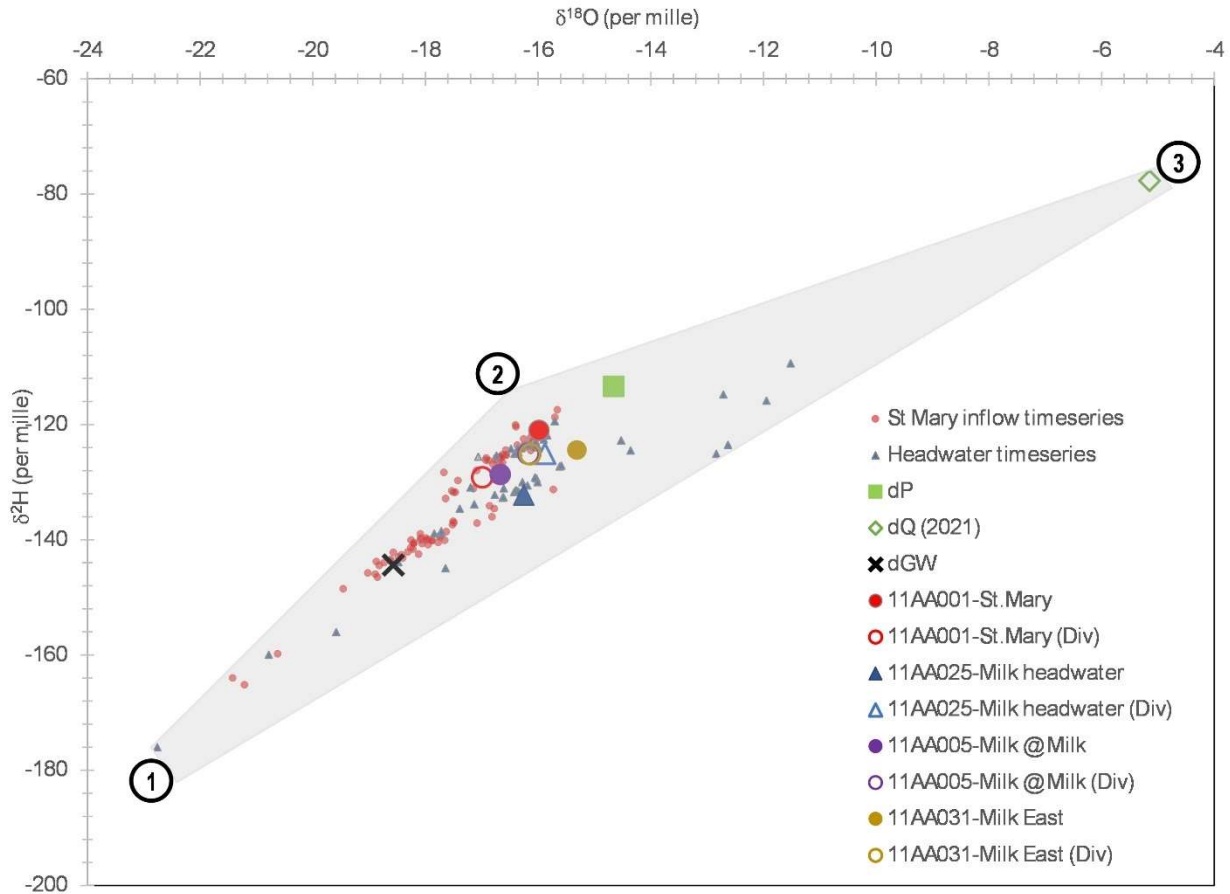


Figure 18. EMMA mixing regime for water isotopes collected from different SMM source waters. The gray region denotes the mixing regime; end points are denoted by 1, 2 and 3 (red numbers). Solid markers represent all data, while hollow represent diversion-affected only (May to September).

The corners of the envelope are defined by three endpoints: 1) depleted precipitation (snow) and groundwater, 2) St. Mary inflows, and 3) enriched summer runoff. Transect 1-3 tracks the enrichment of headwater samples (11AA025) from seasonal snowmelt and baseflow to evaporatively-enriched runoff, while transect 2-3 tracks the isotopic evolution of summer precipitation into enriched summer runoff, or the natural seasonal behaviour of the Milk River system. The headwater streamflow samples (blue triangles) achieve close to the most enriched streamflow end point (3).

Transect 2-1 controls the influence of the diversion inflow on the isotopic composition of the Milk River system, pulling the non-diversion season (closed circles) streamflow samples toward end point 1 when the diversion is active (open circles), which is counter to the natural behaviour of the system as indicated by the Milk River headwater (HW; closed triangle to open triangle) during the same seasonal periods. The diversion acts to deplete the Milk River streamflow, shifting the isotopic composition closer to the groundwater composition (X). The proximity of groundwater (X) and end point 2 within the mixing envelope is notable, supporting the origin of St. Mary streamflow as primarily derived from long-term average

precipitation (snow and rain), but also presents a challenge when applying EMMA to separate diversion inflow and the groundwater endmember. Moving downstream in the Milk River system, the isotopic composition is pulled into the centre of the mixing envelope and further away from end point 2, indicating a diminishing influence of the diversion and groundwater.

Based on hydrometric water balance, there is an on average 3 m³/s underestimation of streamflow at Milk River (11AA005, C) assuming the sum of 11AA025 (A) and 11AA001 (B) should yield total flow at C. This suggests that flow balance alone cannot account for diversion inflow. This analysis required simultaneous flow and isotope data at all three locations on the same or close to the same day – there were very few periods where this occurred, and only in 2018 and 2023. Isotopically, it is estimated that the Canadian Milk River receives, on average (2018 and 2023 data only available), 9.3 m³/s (329 ft³/s) of diverted inflow during the diversion season.

EMMA was also applied exclusively to the diversion season to estimate the relative contribution of diverted inflow to the Milk River system relative to other sources using isotope separation methods (Table 9). This analysis reveals that approximately 93% of total downstream eastern crossing flow is diversion inflow during the diversion season, with <7% being local runoff. Mid-reach (11AA005) is similarly dominated by diversion inflow (96%) relative to local runoff (4%). The headwater region is approximately 82% groundwater reliant, and 18% direct runoff (exposed to surface evaporation), which means that groundwater recharge (and local snowpacks) are critical elements for headwater water balance. Due to the similarity between diversion inflow and groundwater isotope signature, the downstream separation of groundwater and diversion inflow components is less certain but suggests 70% groundwater and 30% diverted inflow. Assessing the accuracy of this final separation unfortunately requires physically based, continuous modelling of both baseflow and diversion components, however, to verify.

Table 9. EMMA results, estimating the contribution of diversion inflow from the St. Mary to total streamflow relative to a second endmember while the diversion is active. HW = Milk headwater (11AA025), GW = groundwater endpoint, Milk-East = 11AA031, Milk@Milk = 11AA005.

Variable	Component	Fraction, $\delta^{18}\text{O}$	Fraction, $\delta^2\text{H}$	Average (%)	Error (%)
What mixture of GW (1) and evaporated runoff (2) are the Milk HW (T) annually?					
f1	Groundwater	0.828	0.817	82	1
f2	Evaporated δQ	0.172	0.183	18	
What mixture of diversion inflow (1) and local headwater runoff (2) is the Milk-East (T) during diversion season?					
f1	Diversion inflow	0.93	0.92	93	1
f2	Evaporated δQ	0.07	0.08	7	
What mixture of Milk HW (1) and diversion inflow (2) is the Milk@Milk (T) during diversion season?					

<i>f1</i>	Headwater δQ	0.048	0.032	4	34
<i>f2</i>	Diversion inflow	0.952	0.968	96	
<i>What mixture of St. Mary inflow (1) and GW (2) is the Milk-East (T) annually?</i>					
<i>f1</i>	Groundwater δ_{GW}	0.735	0.671	70	9
<i>f2</i>	St. Mary δQ	0.265	0.329	30	

3.3. Water Balance Assessment

Isotope-water mass balance can be used to derive hydrologic ratios informed by changes in water balance components such as transpiration (T) relative to total evapotranspiration (ET) loss, evaporation (E) relative to total basin inflow (P for headwater basins, I for nested downstream basins with upstream contributing streamflow), and water yield (WY), or total runoff for a basin area. In this study, these calculations are applied at the subbasin scale, and only for the open water season (May to October) to correspond to the sampling period for isotopes in streamflow (δ_Q) and the seasonal measurement of streamflow at the gauges.

Further to the EMMA and end-member assessment, analytical isotope modelling was used to estimate water balance components, specifically runoff or water yield (WY), evaporation relative to inflow (E/I) and transpiration (T/ET). Inflow (m^3) is assumed to be the sum of precipitation (P), runoff (R) and upstream inflows (J) in m^3 based on the formulation by Haig (2021):

$$I = P + R + J \quad (12)$$

where P is precipitation (derived from isoP, Section 2.1.1), R is runoff, and J is upstream inflow (Haig, 2018). In headwater basins (here, Basin IDs 1, 2), the inflow is assumed to be the precipitation ($\delta_I \approx \delta_P$). Otherwise, the isotopic composition of inflow is estimated from the mass balance (Basin IDs 3, 4):

$$\delta_I = \frac{P\delta_P + R\delta_R + J\delta_J}{P + R + J} \quad (13)$$

where δ_I , δ_P , δ_R , and δ_J are the isotopic compositions of inflow, precipitation, runoff, and upstream inflow (Haig et al. 2021). To estimate runoff (R), it is assumed that the isotopic composition of precipitation and runoff are consistent ($\delta_P \approx \delta_R$), and minimal isotopic fractionation occurs along the flow path (Glavonijc, 2020). Isotopic composition of runoff, δ_R is derived from streamflow samples ($\delta_R = \delta_Q$). By defining x as the dimensionless ratio of evaporation loss (E) to inflow (I), which can be determined solely from an isotopic mass balance:

$$x = \frac{E}{I} = \frac{\delta_I - \delta_Q}{\delta_E - \delta_Q} \quad (14)$$

By substituting Equation (14) into (12), and solving for runoff, R (m^3) we get:

$$R = \frac{E}{x} - P - J \quad (15)$$

where J is the sum of all the inflows to the sub-basin and δ_j is the flux-weighted averages of the isotopic composition of the upstream basin streamflow. Assuming zero change in water storage (over the time between sampling), the total water balance of a basin (mm) is expressed as:

$$P - N = E + T + Q \quad (16)$$

where P , N , E , T , and Q are precipitation, interception, evaporation, transpiration, and streamflow discharge, respectively. In downstream chained basins (Basin IDs 3 and 4), we apply Equation (13) by assuming $\delta_p \approx \delta_r$ and that groundwater inputs are negligible, along with and acknowledging that surface inflow is subject to evaporation (Haig et al. 2021):

$$\delta_I = \frac{-J\delta_j\delta_Q + E\delta_p\delta_E - E\delta_Q\delta_P + J\delta_p\delta_Q}{E\delta_E - E\delta_Q - J\delta_j + J\delta_p} \quad (17)$$

Evapotranspiration is the sum of evaporation and transpiration ($ET = E + T$) and evaporation is computed from $E = x \cdot P$ in headwater basins (where $I \approx P$). Assuming that interception storage in prairie basins is negligible, then we derive the ratio of transpiration to evapotranspiration, T/ET (Gibson et al. 2021):

$$\frac{T}{ET} = \frac{P - Q - x \cdot P}{P - Q} \quad (18)$$

Results from the water balance assessment are summarized in Table 10 for the Milk River headwater (Basin ID 1), townsite (Basin ID 3) and downstream (Basin ID 4). The North Milk River (11AA001) was not included in this analysis, except to estimate the local flux, J (Equation (15) and inflow composition, δ_i (Equation (17) required for Basin ID 3 calculations.

Water yield (runoff, in mm per year) by subbasin was calculated from isotopic endmembers and hydrometric (streamflow) data for subbasin IDs 1, 3 and 4 (subbasin 2, the St. Mary diversion inflow, was used only to compute local contributions for subbasin 3). Water yield was unsurprisingly the highest in the headwater (subbasin 1) and in the earlier part of the study (2017-2020) and decreased by approximately half from 2021-2024 (Table 10). Subbasin 3 (11AA005) resulted in negative local runoff in some years (2017, 2019) when the sum of inflows to the basin (from 11AA001 and 11AA025) exceeded streamflow observed at this location, assumed to occur from local irrigation withdrawals as negative water yields were small (<4 mm/year; **Error! Reference source not found.**). Subbasin 4 also had negative water yields (2017, 2019, 2022) as the sum of local inflow (from observed flow at 11AA005) exceeded observed flow at 11AA031, presumably also due to local irrigation withdrawals, small to no local inflow, and evaporative water loss along the reach.

Table 10. Water balance assessment summary for average annual basin water yield, E/I and T/ET estimates by year and overall (2016-2024). Basin IDs 3 and 4 are local water balance only (excludes upstream inflows). Dashes represent insufficient data to complete calculations.

Sub-Basin ID	WSC ID	Name	Local Area (km ²)	Year	WY (mm/yr)	E/I	T/ET
1	11AA025	Milk R at Western Crossing of International Boundary	1054				
				2017	46.3	-0.03	1.04
				2018	54.2	0.01	0.99
				2019	56.7	-	-
				2020	55.0	0.19	0.77
				2021	22.3	0.51	0.44
				2022	28.6	-0.10	1.11
				2023	25.6	-0.01	1.02
				2024	17.4	-0.16	1.16
3	11AA005 (nested)	Milk R at Milk R (Local)	1440				
				2017	-3.2	-0.09	1.09
				2018	11.8	0.00	1.00
				2019	-0.6	-0.19	1.19
				2020	2.3	0.06	0.94
				2021	0.9	-0.14	1.14
				2022	2.3	-0.09	1.09
				2023	1.1	-0.18	1.18
				2024	18.89	-0.15	1.15
4	11AA031 (nested)	Milk R at Eastern Crossing of International Boundary (Local)	3793				
				2017	-2.4	-0.15	1.15
				2018	16.7	-0.05	1.05
				2019	-5.8	-0.23	1.23
				2020	1.1	0.10	0.90
				2021	-0.3	-	-
				2022	-3.9	0.45	0.55
				2023	5.5	-0.04	1.04
				2024	2.1	-0.15	1.15

Transpiration was found to dominate annual water loss in all years of the study, consistently accounting for more than half of evapotranspiration losses, and ranging from 0.95 to 1.0 of ET, on average across all subbasins (Figure 19). Several years resulted in a T/ET ratio that exceeded the behavioural threshold of 1.0 when the isotopic composition of streamflow was more depleted than rainfall (δ_P) or the computed inflow (δ_i) composition (Table 10). This likely resulted from the low resolution (monthly) and inconsistency (from streamflow sampling) of isotope in precipitation modelling, or the sporadic and low-resolution sampling streamflow. Errors were small ($T/ET < 1.4$) and despite the magnitude of these partitions being questionable, results indicate a significantly larger fraction of water is lost to transpiration relative to evaporation in all subbasins. The relative water loss, or evaporation relative to inflow, calculations were impacted by precipitation consistently being less than calculated evaporation loss (i.e., $E \gg P$) resulting in a negative water balance, and therefore

negative E/I ratios. The water balance indicates extremely high-water loss, which often exceeds inflow.

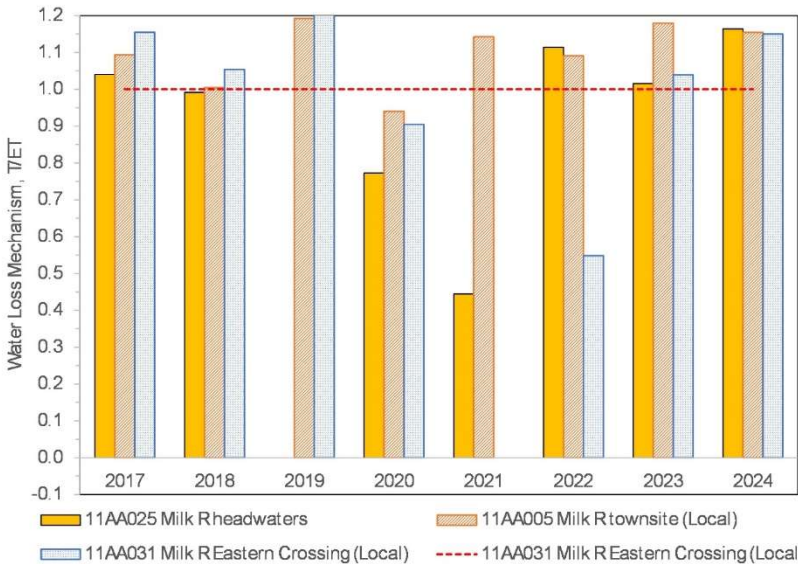
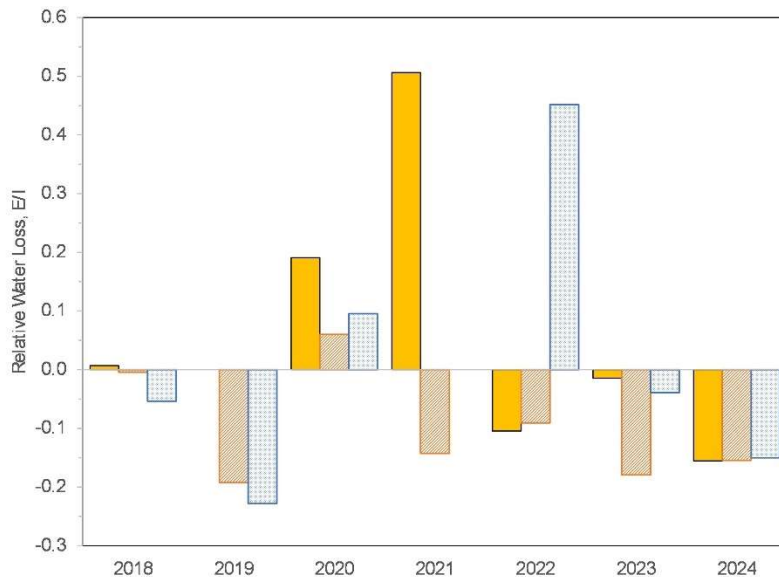


Figure 19. Basin relative water loss derived from isotope-water balance for (a) T/ET, and (b) E/I. Red dashed line represents maximum T/ET physically possible (ratio of 1). Negative values for T/ET and E/I are not physically possible and represent higher local inflow than total inflow, likely resulting from irrigation withdrawals and returns.



Water loss mechanisms (T/ET) and relative losses (E/I) are presented on Figure 19a and **Error! Reference source not found.** Figure 19b, respectively. They frequently exceed physical thresholds of a maximum of 1.0 and minimum of 0.0, reflecting the water balance (Q) discrepancies discussed earlier (Section 3.2.2). T/ET exceeding 1.0 (Figure 19a) is the result of negative evaporation estimated isotopically when the inflow composition or evaporative flux becomes enriched (Equation (15)). The negative evaporation results in a negative E/I ratio (Figure 19b). Though the magnitude of the values may not be trustworthy, the consistency of the results in two credible findings: (1) the Milk River basin ET losses are

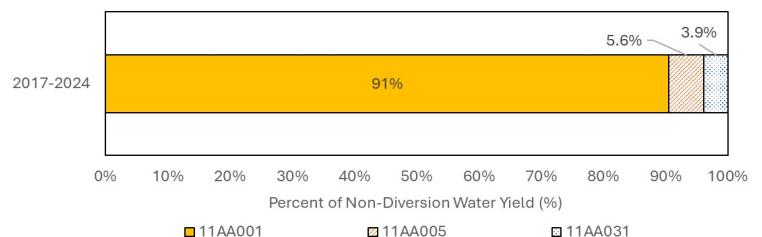
transpiration dominated, and (2) evaporation losses are very small very small evaporative relative to basin inflow.

Unfortunately, the errors in water balance assessment result from the discrepancy in streamwise accumulation of a 3% flow balance error. When downstream flow is less than upstream flow, the isotopic water balance assessment fails. Unless these flow losses can be accounted for and quantified in the water balance, this form of assessment is not viable in the Milk River basin.

4. Summary of Findings

The above results culminate in the following findings about the SMM system, derived from isotope-hydrological analysis:

- Evaporative loss in the Milk is higher relative to the St. Mary basin, naturally.
- Transpiration, as a component of ET, is far greater than evaporative loss in the Milk River basin.
- Milk River headwaters (11AA025) are groundwater-dominated: approximately 82% of total streamflow comes from groundwater annually.
- There is an annual average 3% error in closure of the water balance (from streamflow measurement) at the town of Milk River (11AA005) from 2017-2024: namely, flows at 11AA005 are 5% lower than the sum of their upstream inflows (11AA025 + 11AA001).
- An average annual contribution of 9.34 m³/s (329 ft³/s) of diverted inflow into the Canadian Milk River system is received, based on isotope water-mass balance methods (2018, 2023 only; other years had insufficient data for this analysis).
- During the diversion season Milk River at the town of Milk River (11AA005) streamflow is ~80-85% (up to 96%) diverted inflow, on average (based on data from 2017-2024), relative to only 4% headwater inflow (11AA025).
- Downstream at the eastern crossing (11AA031), the Milk River is estimated to be ~93% diversion inflow, on average (2017-2024).
- Evaporation losses are small (negligible) relative to natural (non-diverted) net basin inflow and transpiration losses.
- Runoff production (water yield) decreases streamwise along the Milk River.



4.1. Gaps in Knowledge

Despite the dedicated three years of monitoring and modelling analyses, gaps in our knowledge and understanding of the Milk River water balance remain related to:

- Observations of isotopes in precipitation to compliment and ground-truth isoP modelled compositions.
- Groundwater is critical in this system, particularly during very low flow, or when the diversion is not active.
- Isotopic similarity of groundwater to St. Mary diversion water makes groundwater separation during the diversion season more uncertain (lower groundwater contributions estimated).
- Role of local runoff (inflow from smaller tributaries that flow year-round) in the southeast of the Milk River basin is relatively uncertain.
- The impact on groundwater partitioning in the downstream (11AA031) reach is also not quantified but important to understand due to these inflows being isotopically depleted (close to groundwater composition).
- EMMA application to estimate volume of diversion inflow is limited by lack of consistent sampling of key gauges (Table 8) *simultaneously* for water balance estimation
- Inconsistencies in the hydrometric water balance moving downstream along the Milk River (annual ~3% underestimation of flow), preventing isotopic analytical assessment from being feasible (Section 3.3).

5. Recommendations

5.1. Value of Isotopes Monitoring

Water balance estimation from streamflow yields a -5% error annually (i.e., at Milk River at Milk River town). **Isotope mass balance offers an alternative assessment method for water balance and diversion inflow estimation.**

- Isotopes when coupled with streamflow data provide assessment of water balance components (E, T, WY or runoff, groundwater). They can answer: *where is flow generated from, how much is there, and how vulnerable are these sources to change?*

Isotope data are most valuable with hydrometric data, and consistent and regular timeseries of both at all key locations afford mixing model separations and diversion analyses.

5.2. Sustaining an Isotope Monitoring Network

A long-term commitment to **an isotope monitoring network in the Milk River could be established at a minimum cost of 2100 CAD/year** (Table 11). Should this network be funded, it is recommended that:

- Establish citizen science sampling with the Milk River Watershed Council Canada (MRWCC). Contact has already been made, and the council is keen to support long-term sampling.
- Establish precipitation isotope sampling at the Milk River Watershed Council Canada (MRWCC) office in the Town of Milk River
- Continue to sample the main transect points from the Milk River headwaters, diversion inflow channel, town of Milk River and some distance downstream to sustain the monitoring network.
- Isotope samples from the eastern crossing are best retrieved by USGS/WSC hydrometric personnel as this site remains rarely sampled and difficult to access for research personnel.
- Connect with Alberta EPA staff about long-term groundwater monitoring reinitiation in this region and continue to update the groundwater isotopic composition based on their data.
- More frequent sampling of the shoulder seasons (outside of the active diversion period) is highly valuable for EMMA modelling.
- Coordinated and consistent (in time) sampling of the key gauges (Table 8) needed to support isotope mass balance mixing models (EMMA) is critical.
- River samples from these gauges are ideally collected a minimum of 7 times per year:
 - Prior to freshet to capture ice-on baseflow (*end of February-early March*)
 - Onset of diversion season (*April*)
 - Summer (*July, August, September*)
 - Just before diversion is shut off (*end of September-early October*)
 - Prior to freeze-up (*early to late November*)
 - Additional sampling in *May and June* is helpful but does not prohibit water balance assessment.

Table 11. Base isotope monitoring sample collection schedule, viable to be supported by WSC/USGS, and associated cost estimate for 2025 and beyond.

No. of Locations	Source	Samples per location per year	Total samples per year	Cost, sub-total (CAD)
2	Groundwater	2	4	\$ 100.00
1	Precipitation	12	12	\$ 300.00
4	Streamflow	12	48	\$ 1,200.00
4	Baseflow	1	4	\$ 100.00

20%	Duplicates	1	16	\$ 400.00
	TOTAL		96	\$ 2,100.00

5.3. Isotope-Hydrological Modelling

A proof-of-concept model of the Milk River basin has been established and tested. **Continuous isotope-hydrological simulation has demonstrated success in achieving water balance partitioning with acceptable accuracy.**

HYPE-MAITsim modelling is promising and demonstrates an excellent test of the hydrological model setup. Results on the process-based accuracy of the hydrological model are mixed, generally:

- Good total flow simulation in the headwater, good summer/winter flow volume, and mixed accuracy for spring freshet (peak flow)
- Total summer evaporative loss agrees with isotope data on evaporative enrichment
- Baseflow contributions are more variable (expected for continuous simulation), and generally agree with EMMA results
- Groundwater composition is stable (good) but much too enriched: either recharge is unrealistically summer biased (it should be winter/early spring biased) or it is too influenced by soil evaporation higher in the soil layers

HYPE simulations be updated to near present day to coincide with the isotope sampling record. Generally, HYPE modelling can be improved by:

- Increasing open water evaporation and decrease soil evaporation (total summer evaporation was reasonably accurate so these need to be balanced)
- Allowing for macropore recharge, where groundwater recharge bypassing the evaporating upper soil layers (i.e., increasing snowmelt recharge ‘directly’ to groundwater is indicated by the isotope simulation)

Isotopes can help improve the hydrological modeling through continuous multi-objective optimization to both streamflow and isotopes. A HYPE sub-model of only the headwaters (where we have isotope data) can be linked to MAITsim directly and calibrated with some minor workflow adjustments (i.e., add the MAITsim R scripts to the iteration loop). Improving the internal process simulation accuracy in this way is particularly relevant to the simulation of projected future flows in this basin. Simulating evaporation from open water versus soil moisture may be affected by projected temperature increases, and capturing the observed winter precipitation bias in shallow groundwater recharge will change simulated baseflow contributions when snowpack accumulation and melt alter.

A proposal for such work was submitted in 2024, which would see a continued minimal investment in an isotope monitoring network and simultaneously advance the coupled isotope-hydrological modelling. This would support improved parameter optimization (for

hydrological modelling projections of climate change), and continuous simulation of climate and diversion scenarios of interest to the IWI Study Board.

6. Data Availability

The MAITsim (Model-Agnostic Isotope Tracer simulation) code is available on GitHub: <https://github.com/tegan-holmes/MAITsim>).

An R-based re-implementation of the UC-HAL isotope-hydrology framework used in this report. IsoHP automates every calculation – data processing, EMMA mixing-model setups, and mass-balance partitioning – in order to rerun analyses with new data or apply the same workflow to a different basin. The project is modular, breaking the workflow into bite-sized R scripts, and is under active development with continuous updates at <https://github.com/Anthony-Kroll/IsoHP>.

An Interactive Isotope Sampling Map

(https://www.google.com/maps/d/edit?mid=1VqTAFvBjZqP7KLJbDZliEzyk_MbpMc&usp=sharing) displays every isotope sampling site used in this study, and each marker's popup provides the site ID and coordinates, the number of samples collected, the sampling group responsible, and the date range during which those samples were taken.

7. References

- Allison, G. B., C. J. Barnes, and M. W. Hughes. 1983. "The distribution of deuterium and ^{18}O in dry soils 2. Experimental." *J Hydrol (Amst)*, 64 (1–4): 377–397. Elsevier. [https://doi.org/10.1016/0022-1694\(83\)90078-1](https://doi.org/10.1016/0022-1694(83)90078-1).
- Delavau, C., K. P. Chun, T. Stadnyk, S. J. Birks, and J. M. Welker. 2015. "North American precipitation isotope ($\delta^{18}\text{O}$) zones revealed in time series modeling across Canada and northern United States." *Water Resour Res*, 51 (2): 1284–1299. John Wiley & Sons, Ltd. <https://doi.org/10.1002/2014WR015687>.
- Gibson, J. J., T. Holmes, T. A. Stadnyk, S. J. Birks, P. Eby, and A. Pietroniro. 2021. "Isotopic constraints on water balance and evapotranspiration partitioning in gauged watersheds across Canada." *J Hydrol Reg Stud*, 37: 100878. Elsevier. <https://doi.org/10.1016/j.ejrh.2021.100878>.
- Haig, H. A., N. M. Hayes, G. L. Simpson, Y. Yi, B. Wissel, K. R. Hodder, and P. R. Leavitt. 2021. "Effects of seasonal and interannual variability in water isotopes ($\delta^2\text{H}$, $\delta^{18}\text{O}$) on estimates of water balance in a chain of seven prairie lakes." *J Hydrol X*, 10: 100069. Elsevier. <https://doi.org/10.1016/j.hydroa.2020.100069>.

- Horita, J., K. Rozanski, and S. Cohen. 2008. "Isotope effects in the evaporation of water: A status report of the Craig-Gordon model." *Isotopes Environ Health Stud*, 44 (1): 23–49. <https://doi.org/10.1080/10256010801887174>.
- Welhan, J. A., and P. Fritz. 1977. "Evaporation pan isotopic behavior as an index of isotopic evaporation conditions." *Geochim Cosmochim Acta*, 41 (5): 682–686. Pergamon. [https://doi.org/10.1016/0016-7037\(77\)90306-4](https://doi.org/10.1016/0016-7037(77)90306-4).